THE ELECTROPHYSIOLOGICAL EFFECTS OF BLOCKADE OF THE NON-SPECIFIC THALAMUS UPON SENSORY RESPONSES IN THE POSTCRUCIATE CORTEX OF THE CAT

by

Stuart M. Rosenblum

A THESIS

Presented to the Department of Medical Psychology
and the Graduate Division of the University of Oregon Medical School
in partial fulfillment of
the requirements for the degree of

Master of Science
June, 1974

APPROVED:

[redacted] . . . . . .

Professor in Charge of Thesis

[redacted] . . . . . .

Chairman, Graduate Council

To Judy,
with all due respect
to Fido

"I feel like the child
standing on tiptoes
to see over the
mountain."

JS

TABLE OF CONTENTS

ACKNOWLEDGEMENTS

I would like to acknowledge the assistance of those individuals that made this study possible. Dr. James O'Brien was the foremost influence in guiding this study. His time, effort, and suggestions were invaluable. This study was accomplished using his laboratory facilities. I am indebted to my thesis committee for their assistance. The histology was accomplished with the assistance of Dr. Vaughn Critchlow. I am indebted to Jessie Kroning and Vicki Stites for help in preparing the histological material. Both Dr. James O'Brien and Daniel Gray have assisted with their computer programming skills. I am also indebted to Dr. John Brookhart for his helpful advice.

LIST OF TABLES

LIST OF FIGURES

INTRODUCTION

Knowledge about the contribution of the non-specific sensory system to sensory evoked activity of the cortex has remained very limited in comparison to what is known about the specific sensory pathways. A distinction has classically been made between the specific thalamo-cortical system and that which has been variously described as unspecific, generalized, multisensory, or non-specific (21). While the specific thalamo-cortical system is characterized by high fidelity of transmission and precise structural (35) and functional organization (29), the non-specific thalamo-cortical system is usually considered to perform a diffuse energizing function (29). The belief that the non-specific thalamic nuclei may be viewed as a dorsal elaboration of the brainstem reticular formation is consistent with such a diffuse energizing function.

Although there is less than unanimous agreement as to which thalamic nuclei should rightly be considered non-specific, it is evident that the centromedian-parafascicular (CM-PF) complex falls within this category, as well as the other intralaminar and midline nuclei. As initially described by Morison and Dempsey (27), low frequency stimulation within the non-specific nuclear mass yields the characteristic waxing and waning of amplitude of the cortical recruiting responses (18). The non-specific nature of sensory input to CM has been shown by the existence of polysensory unit responses (1). However, CM is somewhat atypical of the non-specific thalamic nuclei in its increasing importance phylogenetically. The CM component of the CM-PF complex is virtually absent in the mouse and achieves its greatest size in the primates (36).

Centromedian occupies a critical position in the caudal thalamus. Immediately caudal to the CM-PF complex, the ascending fibers of the brainstem reticular formation bifurcate into a dorsal and ventral leaf (35). The dorsal lamella proceeds through the intralaminar and dorsomedial thalamic fields, possibly as far rostral as the reticular nucleus. At the CM bifurcation, the ventral leaf proceeds ventral and lateral through the subthalamus and hypothalamus. According to the Scheibels, collaterals extend from the bifurcated ascending fibers to terminate upon postsynaptic elements of the CM field (36).

According to Bowsher, the gigantocellular reticular nucleus of the lower brainstem is a relay to CM for spinal afferent impulses evoked by somatic stimulation (10). The author suggests that this spinocentromedian path is the most important ascending afferent projection, although additional afferent pathways comprise the "paleospinothalamic system." The electrophysiological studies of this gigantocellular bulbar relay to CM are consistent with the polysensory nature of CM units (9).

Petras, studying lesions in the motor cortex, demonstrated massive fine-fibered terminations that distribute throughout CM (26). This cortical pathway provides an anatomical basis for a modulating effect which the cortex might exert on CM.

In analogy with the thalamo-cortical systems, the corpus striatum has efferent as well as afferent connections with CM and other nonspecific thalamic nuclei. Efferent fibers to CM from the globus pallidus have been described (26). In addition, Nauta and Whitlock have confirmed a projection from CM to the putamen (30).

Anatomical information has not been conclusive in describing the efferent projections of the centromedian-parafasicular complex to the cortex. Some of the discrepancy in the literature can be attributed to the problems inherent in the techniques. Walker (50) is representative of a goup of anatomists who concluded that there is no direct projection from CM to the cortex, as evidenced by retrograde degeneration studies. Such degeneration studies would be misleading if thalamic cells have collateral branches to more than one cortical area or to both the cortex and subcortical structures, and if collateral projections could maintain the cell function. This criticism is especially relevant since the Golgi method studies by Scheibel and Scheibel demonstrate the extensive collateral patterns generated by the axons of the intralaminar nuclei (36).

Anterograde degeneration studies suggest the existence of fibers between the CM-PF complex and the frontal and parietal cortical areas. Bowsher found that subsequent to CM lesions, degenerated efferent fibers were seen passing rostrodorsolaterally through adjacent ventral and lateral thalamic nuclei, eventually passing as discrete bundles into some of the white stalks of the cortical mantle (9). However, Nauta and Whitlock, although reaching the same conclusion, tempered their findings with the realization that an inherent difficulty in this technique is the uncertainty as to whether degeneration might have arisen from interference with fibers of passage (30). Similarly, Golgi material has not given definitive answers to the problem of the projection from the posterior half of the nonspecific system since frequent changes in the plane and direction of these fibers make plotting their course difficult.

The rationale for studying the post-cruciate cortex is based upon electrophysiological findings. A considerable amount of sensory convergence can be demonstrated in the post-cruciate cortex as reflected by the high proportion of polysensory cells. Additionally, single pulse electrical stimulation of CM can evoke responses in the post-cruciate cortex.

Buser described the large proportion of polysensory neurons isolated in the immediate vicinity of the cruciate sulcus. Approximately 92% of the units immediately posterior to the sulcus were responsive to at least two sensory modalities. Extending further posterior the proportion of polysensory cells decreased rapidly (13).

O'Brien and Fox further substantiated the polysensory nature of the post-cruciate cortex of the cat. Using an auditory click, light flash, somatic stimulation and brain-stem stimulation, 89% of the cells of the post-cruciate cortex responded to two or more stimuli. Fifty-seven percent of the cells were multisensory with respect to click, light, and somatic stimulation (31, 32).

Blum et al. investigated the ability of stimulation of various sites to elicit responses in neurons of the postcruciate cortex. While they did not find any antidromic unit responses due to CM stimulation, they did obtain units that responded orthodromically to CM stimulation. Both pyramidal as well as non-pyramidal tract neurons were encountered that did respond to single pulse CM stimulation. These unit responses were often securely stimulus bound and had little variability of latency. The authors found evidence of convergence of input in the post-cruciate

cortex from CM and additional stimulation sites. These sites include the ventrolateral nucleus of the thalamus and the primary sensory receiving area (8).

One strategy for studying the sensory information contributed by the non-specific thalamus to the cortex is to impair the functional system with a lesion. Cooling lesions have been used to temporarily and reversibly block regions of the thalamus.

Skinner and Lindsley used a reversible cryogenic blockade in the region of the inferior thalamic peduncle (ITP), the pathway interconnecting the frontal granular cortex and the medial thalamus. They found enhancement of the short latency sensory evoked potentials, as elicited by stimulation of the cochlear nucleus, the optic tract, and optic radiations. According to the premise that the large first and small second positive deflections of the visual EP are geniculocortical of origin and that the third and fourth deflections are cortical, Skinner proposed increased responsiveness both at the level of the thalamus and cortex during ITP blockade. This conclusion was derived from the differential effect of ITP cooling with respect to optic tract stimulation and optic radiations stimulation (45).

Skinner found comparable enhancement of the visual and auditory evoked responses, suggestive of the complete nonspecificity of this thalamo-cortical system with regard to modality (45). However, Benita and Conde (5) and Albe-Fessard (2) have found different results for somatic stimuli. Using a thalamic cooling blockade in the region of CM, Benita and Conde reported that there was no effect on the short

latency responses to somatic stimulation. In contrast, Albe-Fessard found the abolition of somatic evoked activity during CM cooling.

This study was, therefore, designed to examine the sensory evoked activity in the postcruciate cortex contributed through the non-specific thalamus. The contributed sensory activity will be characterized both qualitatively and quantitatively. It remains to be answered whether the sensory activity ascending from the centromedian area of the thalamus to the postcruciate cortex is completely non-specific or whether there are differences with regard to modality. In addition, it is the aim of this study to examine in a quantitative manner the magnitude of contribution to the cortical responses and the time course of the sensory contribution. Thus, it can be determined whether any particular temporal portion of the response predominantly reflects the non-specific thalamic contribution of sensory information.

Cryogenic technique

It was deemed advantageous to use a technique for producing reversible functional blockade, rather than permanent lesioning. Such a procedure allows a comparison with controls, both before and after the cooling procedure, enabling an analysis of the effects specifically related to the experimental procedure. Various methods have been used to render neural tissue temporarily inactive, including disruptions caused by chemicals (25, 42), anoxia (25, 42), pressure (25), ultrasound (4, 25), warming (25, 42), and cooling (2, 6, 20, 25, 42). The cooling technique seems particularly suitable for subcortical blockade. Advantages include rapid reversibility, the localization of the functional blockade, and a minimum of permanent damage.

Previous studies have shown a restricted temperature gradient around the cryoprobe tip inserted in a brain at 37° C. or in an agar medium (16). Skinner reported that cryogenic blockade of the inferior thalamic peduncle did not interfere with conduction of fibers in the adjacent part of the internal capsule (43). Thus, the effective temperature gradient is limited to a few millimeters from the cryoprobe tip when the probe temperature is stabilized at 10° C. It is evident that the volume of the functional blockade is most directly related to probe temperature. Skinner suggested that the functional blockade extends 2-3 mm from the probe tip when the cryoprobe temperature is stabilized at 0° C. (44).

The effective cooling gradient is influenced by the local cerebral vasculature, acting as a heat source. Thus, the volume of tissue subjected to blockade is dependent upon the site of cooling. It is possible that with differing vasculature the temperature gradient associated with topical cortical cooling would differ from that associated with subcortical cooling (28).

The extent of the functional blockade is not only determined by the physical temperature gradient, but by the sensitivity of the neuronal processes to disruption by cooling. It is well established that lower temperatures are required to block fiber conduction than synaptic activity. Mammalian A fibers can be reversibly blocked at temperatures of 5-6° C., while smaller fibers require lower temperatures (15). Conduction along C fibers is disrupted at 0° C. (24).

Synaptic processes are more sensitive to decreased temperatures than fiber conduction. Several laboratories have observed blockade

of cerebral synaptic processes at temperatures in the vicinity of 20° C. Jasper reported that the local direct cortical response could be blocked by cooling to approximately 20° C., reflecting disrupted neuronal activity among the most superficial cortical synapses (20).

The blockade of cerebral synaptic processes in the vicinity of 20° C. has been observed by other investigators. Dondey, using a subcortical cooling probe, reported the blockade of conduction through nucleus ventralis posterior of the thalamus (16).

Andersen reported that the cerebral cortex could be completely deafferented by cooling the thalamus to 20° C. (3). Benita and Conde used the differential sensitivity to decreased temperature to selectively block synaptic processes while leaving fiber conduction intact (6).

The careful regulation of cooling has been chosen as a technique for blocking synaptic activity of thalamic nucleus centromedian without interfering with the interspersed fibers of passage. The temperature of the cooling probe was stabilized at 5° through 10° C. to achieve as large a volume of tissue blocked as possible, without blocking small fiber conduction. In assuming a temperature gradient of approximately 6° C/mm (20), it is possible that synaptic blockade, at 20° C., would extend across the interpeduncular tract into nucleus parafascicularis. However, the shape of the blockade would not be a simple spheroid, but rather would be influenced by the geometric shape of the cooling probe tip. The shape of the blockade would approximate an ellipsoid, reflecting the irregular geometry of the cooling surface.

Aim of study

The aim of this experiment was to examine the effect of a cryogenic blockade of the caudal non-specific thalamus upon sensory responses recorded from the sensori-motor cortex of the cat. Cortical recordings were made by a micro-electrode in the postcruciate region. Both well distinguished single cell action potentials and evoked potentials were recorded simultaneously from the same recording electrode. Additional data consisted of slow wave activity recorded from a specific sensory nucleus of the thalamus, ventralis postero-lateralis (VPL), and from the surface of the suprasylvian cortex. Since cooling was to be localized within the caudal non-specific thalamus, the extent of cooling spread was monitored by an examination of the VPL evoked potential. The sensory responses investigated included those to visual, contralateral hindlimb subcutaneous shock, and ipsilateral hindlimb subcutaneous shock. To obtain information which might be extrapolated to the awake organism, general anesthesia was not used during data collection.

METHODS

Animal preparation

Experiments were performed on acutely prepared cats with operative procedures performed under ether anesthesia. The surgical procedures included placement of the endotracheal tube, cannulation of the saphenous vein, and mounting the subject in the stereotaxic apparatus. After a complete midline incision in the scalp and retraction of the temporal muscles with a periostial elevator, all cut surfaces were infiltrated with procaine. Using stereotaxic coordinates, five burr holes were made in the skull. After cutting through the dura, the cooling probes and recording electrodes were lowered into position. Liquid agar was placed into the skull openings to re-establish a closed pressure system. Subsequent to electrode placement, ether anesthesia was terminated and gallamine triethiode (Flaxedil) administered for immobilization. Artificial ventilation was maintained at 26 strokes per minute with stroke volume varied to maintain 3.6 - 3.8% tracheal CO_2 levels as monitored on a Godart capnograph.

In preparation for the delivery of subcutaneous electric shock, 21 gauge hypodermic needles were introduced into the paw pad region of the right and left hindlimbs. In preparation for presentation of a light flash stimulus, the nictitating membranes were clamped with the stereotaxic eye bars, and atropine sulphate applied to the cornea to maintain pupil dilation. Body temperature was monitored and maintained at 36 - 38° C. with a heating pad and hot water bottles. Procaine was administered every 4 hours to maintain local anesthesia. Flaxedil was administered either by manual injection or by perfusion pump at the rate of 20 mg per hour.

Cooling blockade procedure

A description of the cooling probe (cryoprobe) has been published (38). The cryoprobe system enables localized cooling at the tip of the probe. Briefly, the cryoprobe functions by the regulated flow of a coolant, cold ethyl alcohol, under pressure through a "U-tube" cryoprobe. A DC heater wire is wrapped around the shaft of the probe, leaving 2 mm bare at the tip. The DC current is supplied by two automobile storage batteries. It was found beneficial to isolate the heater current circuit from the temperature monitoring circuit. The DC current does not interfere with the electrophysiological recording. The amount of current supplied to the heater circuit was regulated using a power transistor, and directly read from an ammeter. The drawing of approximately two amperes of heater current through the low resistance circuit maintained the shaft near body temperature. The temperature of the shaft was maintained between 30° and 36° C. A comparator circuit was utilized to terminate heating if the temperature exceeded 36° C., which prevented irreversible coagulation. In practice, the heater current and alcohol flow were exceedingly stable, and once established would remain constant for the experiment's duration.

The temperature of the tip and shaft of the cryoprobe was continuously monitored via appropriately placed microthermocouples (0.12 mm in diameter). Temperature measurements were accomplished using two copper-constantan junctions. Maintaining one junction at a known reference temperature, the temperature of the second junction could then be determined. The small voltage generated by the opposed junctions was approximately a linear function (40 u V/C°) of the

temperature difference between the monitoring and reference junctions. It was found most convenient to use room temperature as the reference temperature. The temperature within the walk-in experimental chamber was occasionally measured to assure a proper reference value. The reference junction was coated with dental acrylic to eliminate slight fluctuations in air temperature. By calibrating the deflection of a meter with respect to the voltage generated by the difference between the two junctions, the temperature was read directly.

To avoid irreversible damage, cooling below 0° C. was prevented through the use of a comparator circuit. Tip temperature was maintained at 5° C. during cooling. Temperature fluctuations did not exceed ± 2° C.

Cooling blockade sites

Two cryoprobes were placed in the region of the centromedian nucleus of the thalamus with one cryoprobe in each hemisphere. The stereotaxic coordinates used were AP: +7.5 mm, lateral: +2.5, vertical: 0.0 according to Jasper and Ajmone Marsan (19). The locations were verified histologically (Table 1).

Recording electrodes

The largest burr hole exposed the peri-cruciate cortex using stereotaxic coordinates of AP: +21 and Lateral: 2.0. The micro-electrodes were either (1) glass micropipettes filled with 3M NaCl and having approximately 1 u tip diameter, (2) glass coated tungsten, tip 1-2 u, or (3) insulated wire electrodes with a small, 25 u diameter glass coated platinum alloy wire tipette. The micro-electrode was guided until the tip penetrated the cortex, the point of entry being inside the boundaries of 2 mm lateral from the midline and 2 mm

posterior to the sulcus. After penetration of the cortex the burr hole was filled with agar. Additional adjustment of the micro-electrode was accomplished using a hydraulic drive, calibrated in microns. The micro-electrode was lowered until a single cell of appropriate signal-to-noise ratio could be isolated, allowing unequivocal counting of single cell spikes. A cortical screw, used for electrocorticogram recordings, was occasionally placed into the skull and lowered to the dura above the suprasylvian gyrus (AP: 5.0, L: 10.0).

Additionally, a bipolar macro-electrode of .01 stainless steel wire, tip separation 1 mm, one-half mm bared, was placed in nucleus ventralis postero-lateralis (VPL). The stereotaxic coordinates were AP: 9.5, lateral: 7.0, and vertical: 0.5, the exact vertical placement was determined by monitoring the evoked potential elicited by cutaneous shock to the contralateral paw while positioning the thalamic electrode. The temporal muscle of the scalp was used as the reference for the micro-electrode and cortical screw monopolar recording.

Histology

Upon termination of the experiment, the cats were sacrificed using sodium pentobarbital (Nembutal), and the brains were removed and placed into 15% formalin solution. The brains were kept in this solution as long as possible to insure fixation. The thalamic area was prepared with the right hemisphere identified, and was frozen with carbonic ice. Fifty through seventy-five micron thick sections were prepared using an American Optical Company, Model 860 microtome. Every serial section of the probe tracts was placed into water and mounted, being mounted two

sections per slide. Staining was accomplished using toluidine blue. Occasionally luxol fast blue was utilized to aid fiber identification.

Recording procedure

The signal from the micro-electrode was led through a Bak cathode follower, amplified by Tektronix 122 amplifiers and filtered. The frequencies between 0.2 and 50 Hz comprise the evoked potential data, while the frequencies between 400 Hz to 3 KHz comprise the single cell data. Both the single cell data and the evoked potential data were led into amplifiers with adjustable gain. A signal of 1 V peak-to-peak was recorded on a Sangamo FM magnetic tape recorder, and maintained as the data record. Other channels of the magnetic tape contained a time zero marker signal, and the 1 V peak-to-peak signal of the thalamic electrode. Recorded data was continuously monitored on an oscilloscope to assure a clearly distinguishable single cell spike. Additionally, the various 1 volt signal inputs into the Sangamo tape recorder were led into a Grass Instruments electroencephalograph for continuous monitoring of all data channels.

Stimulation apparatus

Weak shock was delivered to the right or left hindlimb by means of 21 gauge hypodermic needles placed subcutaneously in the paw pad region. The shock was less than 10 volts and was delivered by a Devices MK IV isolated stimulator as 4 pulses of 0.5 msec duration at a frequency of 280 Hz. The temporal occurrence of the peripheral stimulation was regulated by a Digitimer crystal clock.

The light stimulus was a single flash from a Grass PS2 photo-stimulator at maximum intensity setting #16. The light was presented 3 feet in front of the cat.

Experimental design

After both cryoprobes and the recording electrodes had been positioned, the micro-electrode was hydraulically lowered in the cortex with a micro-drive until a single cell spike could be isolated. The depth of the electrode from the cortical surface was noted. A stimulus was chosen from the three possible stimuli: (1) contralateral peripheral shock, the left hindlimb; (2) ipsilateral peripheral shock, the right hindlimb; or (3) light flash. The sequence was to present 105 trials of the selected stimulus, at the rate of one stimulus every 3 seconds. The onset of the stimulus was 1 second after the time zero marker signal. The initial 105 trials served as the control period.

The tips of the cryoprobes were then cooled to approximately 5° C., at which time an additional 105 stimuli were presented. Subsequently, cooling was terminated and following temperature recovery, 105 stimulus trials were presented, comprising a post-cooling control condition. Each control or cool condition lasted 5 minutes. Stimuli were not presented during the transition period between the control and cool conditions, but were delayed until the tip temperature had stabilized at greater than 35° C. The transition time was approximately 1 minute.

The sequence of cooling was varied to minimize order effects. In some cases controls were recorded for two different stimuli, then cooling and then second controls and in other cases the sequence was control-cool-control for the individual stimulus.

Data analysis: Evoked potential (EP)

The original data were stored on a Sangamo FM tape recorder in analogue form. The electrocortical potentials and a time zero signal were led into A/D converters of the PDP-12 computer. The time zero marker initiated computer sampling. The amplitude of the evoked potential was sampled every 2 msec starting 10 msec after the stimulus onset. Two hundred and fifty-six sampling addresses resulted in an evoked potential of 512 msec duration.

One hundred trials were added algebraically and the averaged evoked potential (AEP) was stored on LINC tape in digital form. An averaged evoked potential was similarly formed for the one hundred trials of each experimental condition. It was thus possible to compare the averaged evoked potentials for the pre-cool, cool and post-cool conditions.

One method of analysis was a comparison of the peak-to-peak amplitudes. The computer program displayed the ordinate (voltage) value of any selected abscissa (time) value of the AEP. Thus, it was possible to place the cursor on the peak positive and negative deflections and obtain the quantitative difference in peak-to-peak amplitude. The peak-to-peak amplitude was computed using the absolute difference. The abscissa values were selected using the pre-cool control AEP and selecting prominent components. Using the same abscissa values, the cool and post-cool AEPs were quantified for peak-to-peak amplitude. Since shifts in the latencies of the wave forms did not result from cooling, the same abscissa values could be used to measure the peak-to-peak amplitude across conditions. If more than one component was

measured for peak-to-peak amplitude, then that component which was more dynamic across conditions was selected. The latencies of the abscissa values were noted. The response period for which the peak-to-peak analysis was performed is detailed in the individual sections for the sensory stimuli.

The measure of peak-to-peak amplitude assumes that the majority of significant information is conveyed in the peak response. However, a second method for examining the EP data was to integrate the EP waveform, quantifying the area described by the EP (Figure 11), permitting an assessment of the overall neural activity which comprises the waveform. The EP in its original form was transformed, without changing the shape, to provide equal negative and positive area around a zero baseline. The EP waveform was then rectified, giving all positive values, and subsequently integrated. The integrated waveform represents all the area described by the EP waveform which deviates from the mean, in either the positive or negative direction. A quantitative value was then derived of all the area of the EP waveform through 0.5 sec post-stimulus.

A third method of EP analysis examined that interval of the EP which was most affected by the cooling procedure (Figure 11). By superimposing the integrated EP of the control condition with the experimental condition, it was possible to define the interval of the response influenced by cooling. There were typically two portions of the integrated AEPs which could be virtually superimposed, with an aberrant portion between the two (further described under Interval analysis).

Data analysis: Single cell data

Similar to the evoked potential data, the PDP-12 accumulated the single cell data of 100 trials, superimposing the time zero markers, and yielding a post-stimulus histogram (PSH). In this case, the computer recorded the number of occurrences of a spike firing within each 2 msec bin during the 100 stimulus presentations for 512 consecutive bins post-stimulus. It was then possible to consider the mean spike rate during any one trial and during any portion of the response as an instantaneous mean firing rate. Thus, the PSH is a statement of the probability of the firing of a neuron on any one trial at a particular latency.

Firing rate was recorded both before and after the stimulus. One second of data prior to stimulus onset was recorded on each trial, thereby enabling a comparison of post-stimulus rate with pre-stimulus rate. One second of data was stored after stimulus onset, describing the elicited response.

The pre-stimulus mean rate was used as a measure of the stability of the single unit recording. In cases of low noise level and clean spike discrimination, the mean pre-stimulus firing rate was relatively constant. In instances of higher noise level and less easily discriminated spikes, the pre-stimulus rate was occasionally seen to vary. A quality control was instituted which utilized a "z" cut-off score as an operational definition (31, 32). The cut-off score was calculated by the following formula:

$$Z = \frac{\left(\begin{array}{c}\text{mean pre-stimulus spike rate} \\ \text{of the post-cool control}\end{array}\right) \text{ minus } \left(\begin{array}{c}\text{mean pre-stimulus spike rate} \\ \text{of the pre-cool control}\end{array}\right)}{\left(\begin{array}{c}\text{standard deviation of the pre-stimulus spike rate} \\ \text{of the pre-cool control}\end{array}\right)}$$

A z value of 10 was chosen as a cut-off score. Any cell showing a calculated value of 10 or greater was excluded from the data to be further analyzed. Less than 5% of the total number of cells were thus eliminated from the data base.

The post-stimulus response of the single unit was quantified in terms of the mean spike rate. However, it was necessary to consider individually certain periods of the response since most of the cells showed complex post-stimulus histograms (Figures 5, 7, and 9). They exhibited both excitatory components and inhibitory components. Excitatory components are those which exceed the pre-stimulus rate, and inhibitory components are those below the pre-stimulus rate. Consequently, rather than using an a priori, fixed interval for analysis of the post-stimulus response, it seemed preferable to select an interval individualized for each cell. The latter approach would be more sensitive to subtle changes, since a fixed interval might misrepresent the data, such as in the overlap of an excitatory and inhibitory response within the same interval being averaged as the absence of a response. Response components were visually selected with the criterion of selecting as long an interval as possible without combining both excitatory and inhibitory components. The response component selected could have any location in the 1.0 sec period following the stimulus and a duration ranging from 50-300 msec.

Only one component would be selected for any one cell using the pre-cool control. This same interval would then be used for comparison with the cool condition and the post-cool control, measured with respect to the mean firing rate.

RESULTS

Histology

Frozen serial sections were used to examine the placement of the cryoprobes. Histological verification was successfully performed in 16 of the 22 cats and is summarized in Table 1. The histology for 6 cats was lost due to improper procedures, but since the available histology showed consistent cryoprobe placement within the area of centromedian nucleus, the data of these cats were included in the study. For each cat, the placements of the left and right probes were determined. Probe locations were determined by comparing the light projected serial sections with the photographed Nissl stained sections of Snider and Niemer (46). Convenient landmarks used in judging probe placements included the lateral geniculate, habenula, the interpeduncular tract, and the third ventricle. The atlas of Jasper and Ajmone-Marsan, with its schematized outline of thalamic nuclei, was useful for determining the boundaries of CM. The probe tracts were superimposed on the atlas to assess the location and damage associated with each brain.

The AP and lateral coordinate values describe the center of the probe tract; the vertical value describes the tip of the probe. The right hemisphere cryoprobe placement ranged from AP +6.0 mm through +8.5 mm, with a mean of +7.4. Associated with this mean value was a variance of 0.4 mm. The left hemisphere probe placement similarly ranged from +6.0 mm as the most posterior placement through +8.5 mm as the anterior extreme. The mean value was +7.3 mm, with a variance of 0.4 mm. The lateral placements ranged from 2.5 through 3.5 mm from

Table 1: Summary of Cryoprobe Placements*

Cat #	A.P. (Right Probe)	A.P. (Left Probe)	Vertical**	Lateral**
22	7.2	7.2	1.0	2.5
25	6.0	6.0	1.0	2.5
30	7.0	6.5	1.0	3.0
31	7.2	7.5	0.0	3.5
32	7.5	7.5	1.0	2.5
35	8.5	8.0	0.0	2.5
36	7.8	7.8	0.5	3.0
37	7.5	7.5	0.0	3.0
38	7.5	7.5	1.0	2.5
39	7.0	6.8	1.0	2.5
40	8.5	8.5	1.0	2.5
41	7.0	7.0	0.0	2.5
42	7.5	7.5	0.5	2.5
A	8.0	8.0	2.0	2.5
B	-	8.0	1.0	2.5
C	6.5	6.5	0.0	3.0
Mean	7.4	7.3	0.7	2.7
Variance	0.4	0.4	0.3	0.1
Range	6.0 - 8.5	6.0 - 8.5	0.0 - 2.0	2.5 - 3.5

*All coordinates referenced to the atlas of Jasper and Ajmone-Marsan, 1954.

**Both the vertical and lateral coordinates were consistent between the right and left cryoprobes with less variance than in the A.P. dimension. The average value is shown. All placements are in the region of CM which extends from 6.25 through 8.25 A.P. At 7.5 A.P., CM extends from 1.0 through 4.0 lateral and from +2.5 through -1.0 vertical.

the midline, with a mean value of 2.7 mm. The associated variance was 0.1 mm. The vertical placements, describing the position of the cryoprobe tip, ranged from 0.0 through +2.0 mm, with a mean value of +0.7 mm. The associated variance was 0.3 mm.

Occasionally at the experiment's termination, prior to sacrificing the subject, the cryoprobe temperature was lowered below 0° C. In such cases, there was histological evidence of permanent tissue damage, as shown by a large lesion and acellular area. The bilateral cryoprobe tracts of cat #37 are shown in Figure 1. Irreversible damage is evidenced corresponding to the probe dimensions. In contrast with the cases of frozen tissue damage, there was no coagulation apparent along the probe. Excessive tissue damage, adjacent to the probe tip, was not observed when the tip temperature was stabilized at 5° C.

The cryoprobes were oriented in the stereotaxic vertical plane. The irreversible damage associated with the tract corresponded to the physical diameter of the probe, approximately 1.3 mm. Irreversible damage from the probe tract was seen to transect the corpus callosum and corpus fornicis. Tract placement was always lateral to tractus habenulointerpeduncularis. Tract damage was often seen in the descent through the medial aspect of nucleus lateralis dorsalis, the dorsal-medial aspect of nucleus lateralis posterior, and the lateral aspect of the dorsomedial nucleus. There was often some damage to the dorsal aspect of nucleus centromedian; however, in general a large proportion of the nucleus was still intact. In only two cats was the damage to CM as extensive as that shown in Figure 1. The cryoprobe tracts in Figure 2, that of cat #36, show damage to the dorsal aspect of CM, with the bulk of the nucleus intact.

Figure 1. Cryoprobe tracts of cat #37. Magnification 12x.

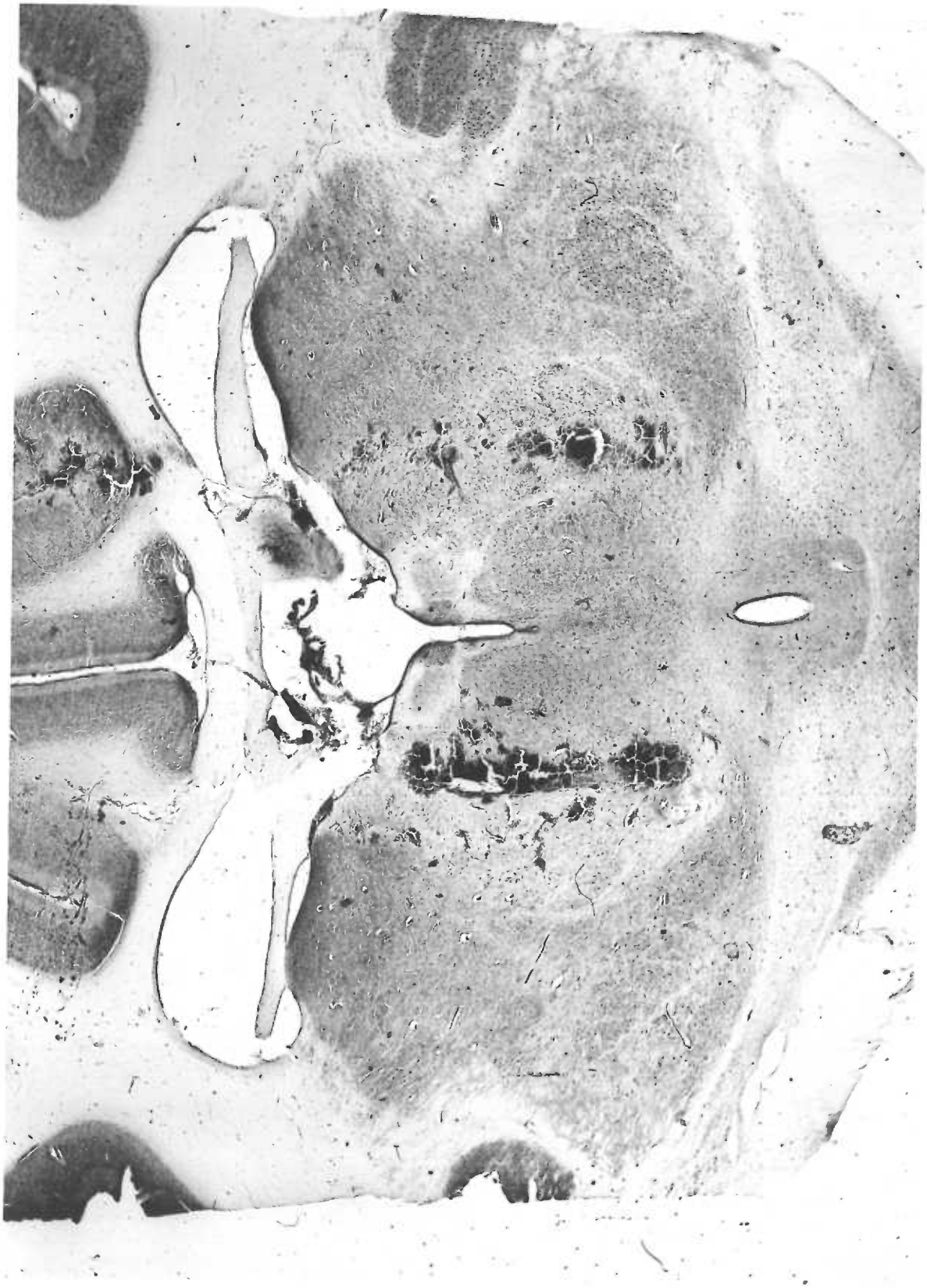

Figure 2. Cryoprobe tracts of cat #36. Magnification 13x.

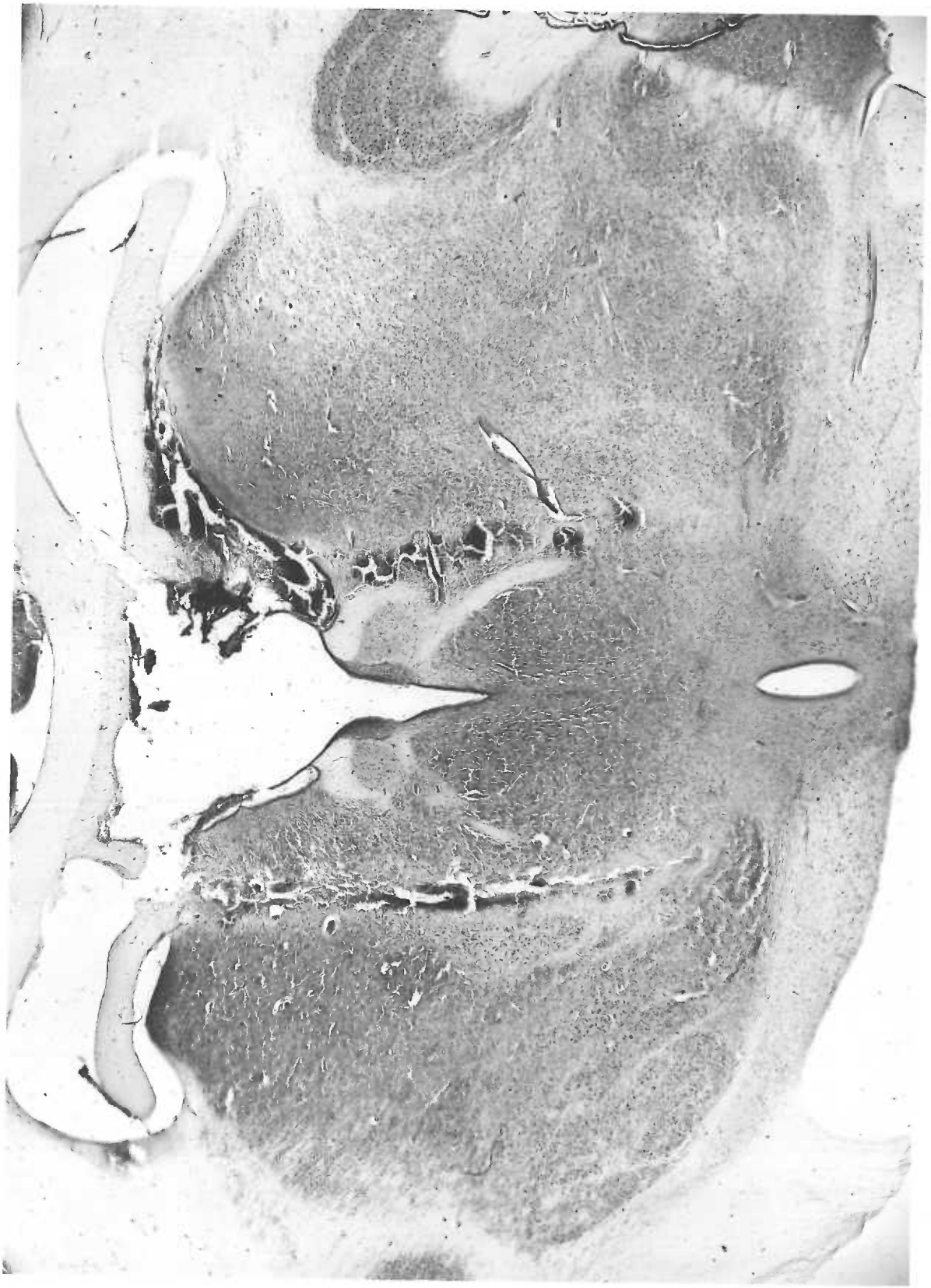

VPL recording

Considering the close proximity of the medial lemniscus and ventralis posterior lateralis (VPL) to the site of cooling blockade, it was important to evaluate the extent of cooling spread. For this purpose a bipolar concentric electrode was placed into VPL in about half of the cats. The placement, accomplished stereotaxically and by monitoring the short latency somatic response, was anterior to the cooling blockade, and could thus demonstrate the integrity of the primary pathway. Figure 3 illustrates a representative case of simultaneous recordings from the VPL electrode and the postcruciate cortex. The short latency response to contralateral paw stimulation recorded from VPL was not affected by bilateral thalamic cooling. The simultaneous recording of the evoked potential in the postcruciate cortex shows a decrease in peak-to-peak amplitude and modification of the longer latency fluctuations.

Single cell data

The single cell data have been separated according to the stimulus and the mode of cooling. Both the pre-stimulus mean rate and post-stimulus rate were examined. On occasion substantial changes were seen in the pre-stimulus mean rate for individual cells. However, the grouped data show that the pre-stimulus mean rate was not significantly affected by thalamic cooling. Figure 4 presents the grouped data for the contralateral paw stimulus with both the pre-stimulus and post-stimulus mean rates graphed. The corresponding values and number of cells are contained in Table 2. A paired *t* test showed that the slight reduction in pre-stimulus mean rate during cooling was not statistically significant

Figure 3. Simultaneous thalamic and cortical averaged evoked potentials. Each trace is the average of 100 trials. Thalamic recording was from nucleus ventralis posterior lateralis (VPL). Focal cortical recording was from the postcruciate cortex.

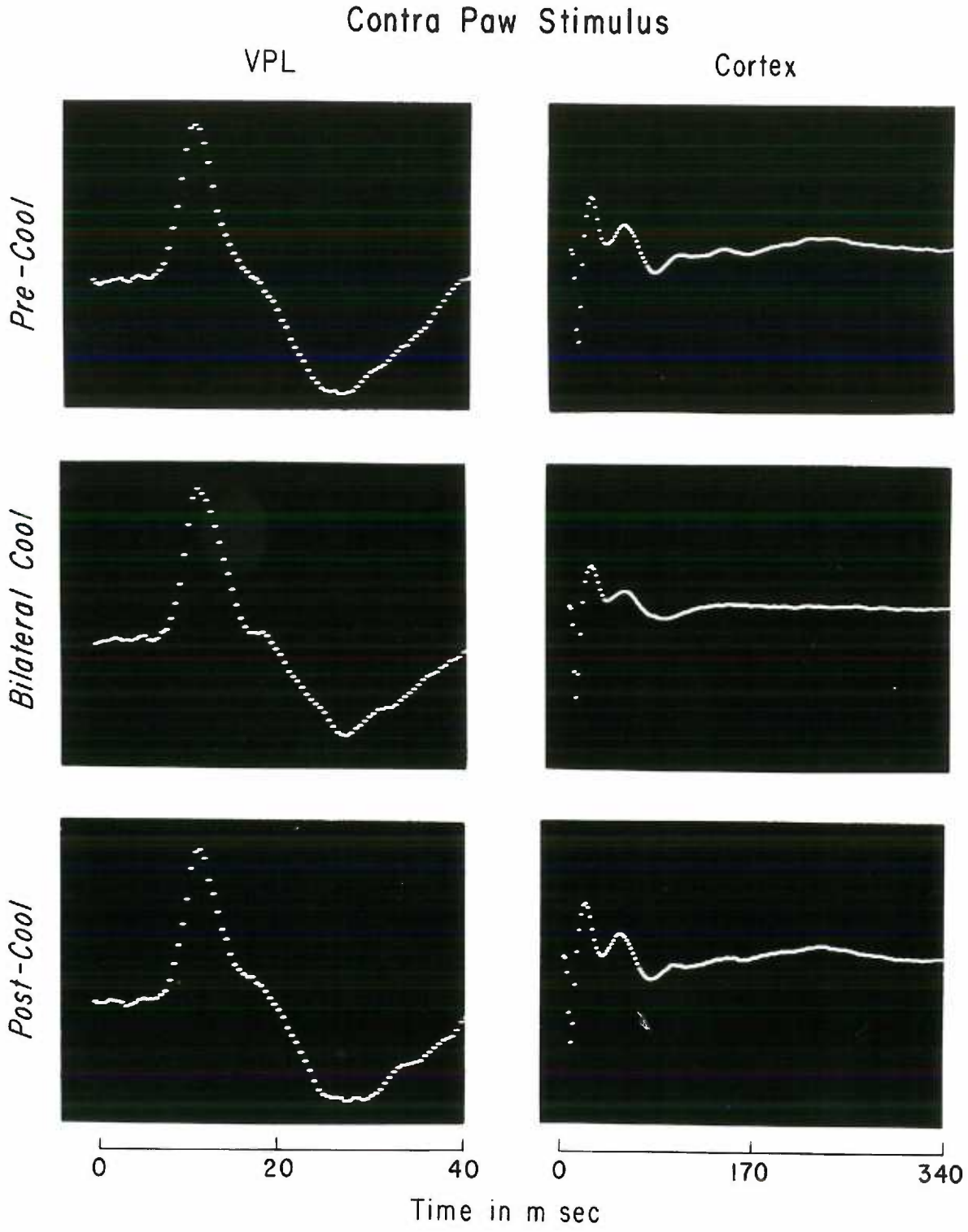
Contra Paw Stimulus
VPL
Cortex
Pre-Cool
Bilateral Cool
Post-Cool
0
20
40
0
170
340
Time in m sec

Figure 4. Relative effect of thalamic cooling on pre-stimulus and post-stimulus spike frequency. The ordinate is the average spike frequency. Responses were elicited by contralateral hindpaw stimulation. For this figure and all subsequent figures, bilateral thalamic cooling is shown by the dotted line, ipsilateral thalamic cooling by the dashed line, and contralateral thalamic cooling by the solid line. Ipsilateral and contralateral are used with respect to the cortical recording site. Excitatory responses exceed the pre-stimulus spike frequency, and inhibitory responses are below the pre-stimulus spike frequency.

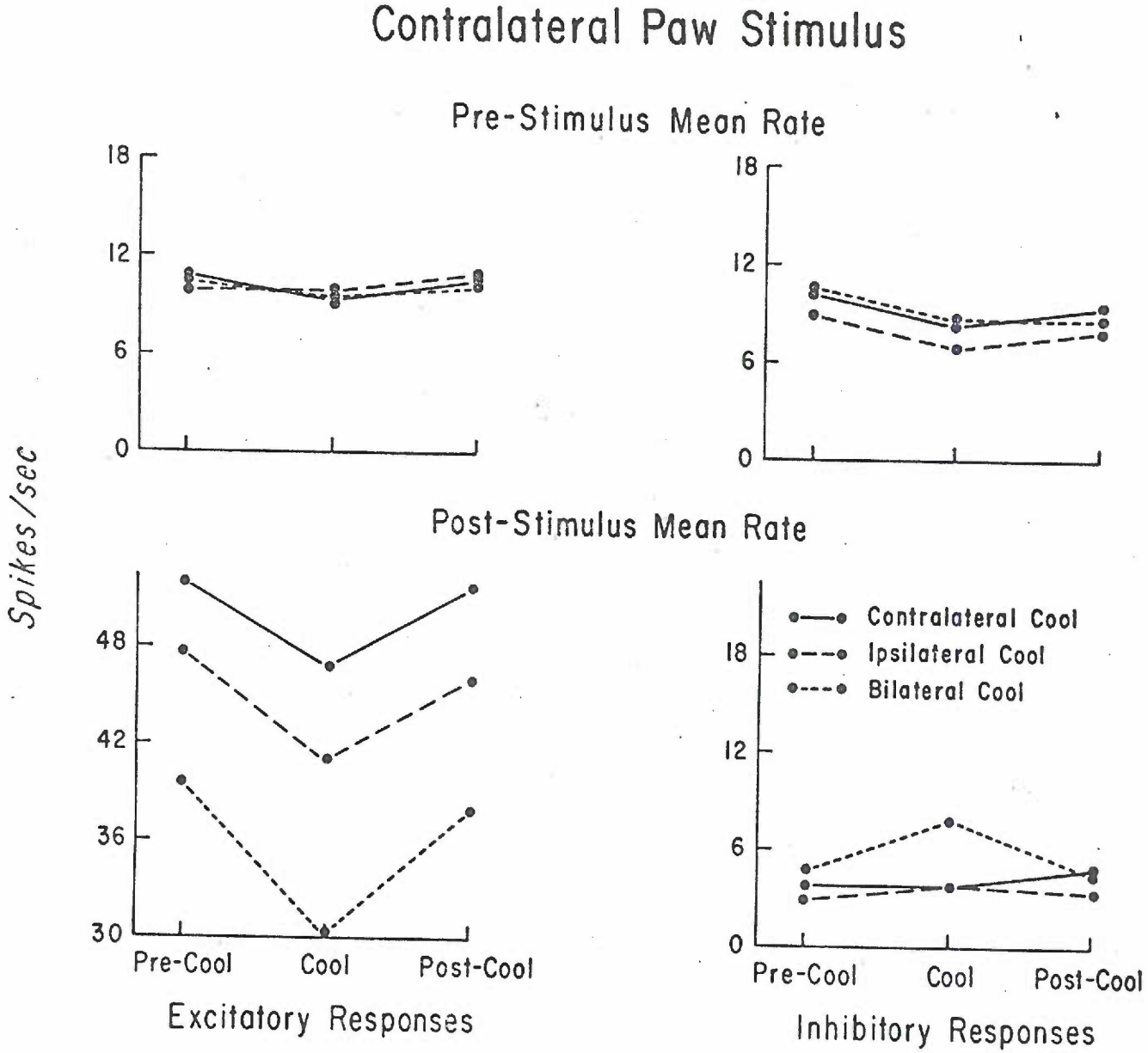
Contralateral Paw Stimulus
Pre-Stimulus Mean Rate
18
12
6
0
18
12
6
0
Post-Stimulus Mean Rate
Spikes/sec
48
42
36
30
Pre-Cool
Cool
Post-Cool
Excitatory Responses
Contralateral Cool
Ipsilateral Cool
Bilateral Cool
18
12
6
0
Pre-Cool
Cool
Post-Cool
Inhibitory Responses

Table 2: Summary of unit responses elicited by contralateral hindpaw stimulation (with respect to pre-stimulus mean rate)

	EXCITATORY RESPONSES			INHIBITORY RESPONSES		
Pre-Stimulus Mean Rate	Pre-Cool	Cool	Post-Cool	Pre-Cool	Cool	Post-Cool
	10.52	9.49	10.30	10.49	8.75	8.66
		Bilat. Cool, N = 32			Bilat. Cool, N = 19	
	11.49	9.88	11.00	8.90	6.81	7.86
		Ipsi. Cool, N = 22			Ipsi Cool, N = 12	
	10.63	9.39	10.59	10.14	8.34	9.36
		Contra Cool, N = 18			Contra Cool, N = 14	
Post-Stimulus Mean Rate	Pre-Cool	Cool	Post-Cool	Pre-Cool	Cool	Post-Cool
	39.53	30.36	37.63	4.77	7.71	4.77
		Bilat. Cool, N = 32			Bilat Cool, N = 19	
	47.77	40.96	45.94	2.92	3.72	3.55
		Ipsi. Cool, N = 22			Ipsi. Cool, N = 12	
	51.94	46.81	51.64	3.67	3.66	4.70
		Contra. Cool, N = 18			Contra. Cool, N = 14	

($p > .05$), while the post-stimulus mean rate changes were highly significant ($p < .01$).

The grouped data for both light and the somatic stimuli showed a tendency for a slight reduction ($p > .05$) in the pre-stimulus mean rate during thalamic cooling regardless of whether the unit response was predominately excitatory or inhibitory (Tables 3 and 4). As might be expected, there was no difference in the effect of thalamic cooling on the pre-stimulus rate on the basis of stimulus placement or modality. Since the pre-stimulus mean rate was not significantly influenced by cooling, the single cell response has been characterized as a difference score, comprised of the evoked mean rate minus the background rate.

Ipsilateral paw stimulation

The effect of cooling CM on an individual cell in the postcruciate cortex is shown in the example of Figure 5. The mean pre-stimulus rate is shown by the stippled area. The excitatory response is that which exceeds the pre-stimulus mean rate, while the inhibitory response is evident below the pre-stimulus mean rate. Unit activity was elicited by stimulation of the ipsilateral hindpaw. The post-stimulus histogram shows a severe decrement in the excitatory components during bilateral thalamic cooling. Inhibitory response components tend to decrease as well, approaching the pre-stimulus mean rate during bilateral thalamic cooling. Recovery of the response, subsequent to termination of cooling, is shown in the lowest histogram.

The grouped data reveal the same pattern. A substantial decrease in the excitatory response components is seen during the cooling procedure (Figure 6). The group mean for the excitatory response rate as

Table 3: Summary of unit responses elicited by ipsilateral hindpaw stimulation (with respect to pre-stimulus mean rate)

	EXCITATORY RESPONSES			INHIBITORY RESPONSES		
Pre-Stimulus Mean Rate	Pre-Cool	Cool	Post-Cool	Pre-Cool	Cool	Post-Cool
	10.68	10.20	10.22	13.38	13.17	11.78
		Bilat. Cool, N = 25			Bilat. Cool, N = 14	
	10.29	8.96	9.94	14.36	11.63	11.29
		Ipsi. Cool, N = 22			Ipsi. Cool, N = 12	
	10.00	9.32	9.59	15.03	12.29	12.87
		Contra. Cool, N = 22			Contra. Cool, N = 11	
Post-Stimulus Mean Rate	Pre-Cool	Cool	Post-Cool	Pre-Cool	Cool	Post-Cool
	26.57	18.12	25.37	6.11	10.59	7.44
		Bilat. Cool, N = 25			Bilat. Cool, N = 14	
	27.66	22.21	26.10	6.69	8.42	7.26
		Ipsi. Cool, N = 22			Ipsi. Cool, N = 12	
	27.11	21.97	25.32	7.17	7.92	7.78
		Contra. Cool, N = 22			Contra. Cool, N = 11	

Table 4: Summary of unit responses elicited by light stimulus (with respect to pre-stimulus mean rate)

	EXCITATORY RESPONSES			INHIBITORY RESPONSES		
Pre-Stimulus Mean Rate	Pre-Cool	Cool	Post-Cool	Pre-Cool	Cool	Post-Cool
	10.73	10.37	10.16	11.40	10.63	10.06
		Bilat. Cool, N = 22			Bilat. Cool, N = 23	
	13.00	12.21	12.60	10.35	8.75	9.97
		Ipsi. Cool, N = 15			Ipsi. Cool, N = 11	
	11.39	11.39	11.06	12.30	11.32	12.36
		Contra. Cool, N = 11			Contra. Cool, N = 13	
Post-Stimulus Mean Rate	Pre-Cool	Cool	Post-Cool	Pre-Cool	Cool	Post-Cool
	13.33	11.39	11.06	9.14	10.76	9.59
		Bilat. Cool, N = 22			Bilat. Cool, N = 23	
	15.56	12.82	14.29	8.70	9.30	9.28
		Ipsi. Cool, N = 15			Ipsi. Cool, N = 11	
	14.26	12.82	12.82	10.98	11.34	11.96
		Contra. Cool, N = 11			Contra. Cool, N = 13	

Figure 5. Post-stimulus histogram of unit activity elicited by ipsilateral hindpaw stimulation and simultaneously recorded averaged evoked potential. Both the histogram and the AEP are summed from 100 trials. Mean pre-stimulus rate is represented as stippled area. The excitatory response (darkened) is that which exceeds the pre-stimulus rate. The inhibitory response is evident below the pre-stimulus rate. No stimulus artefact is present.

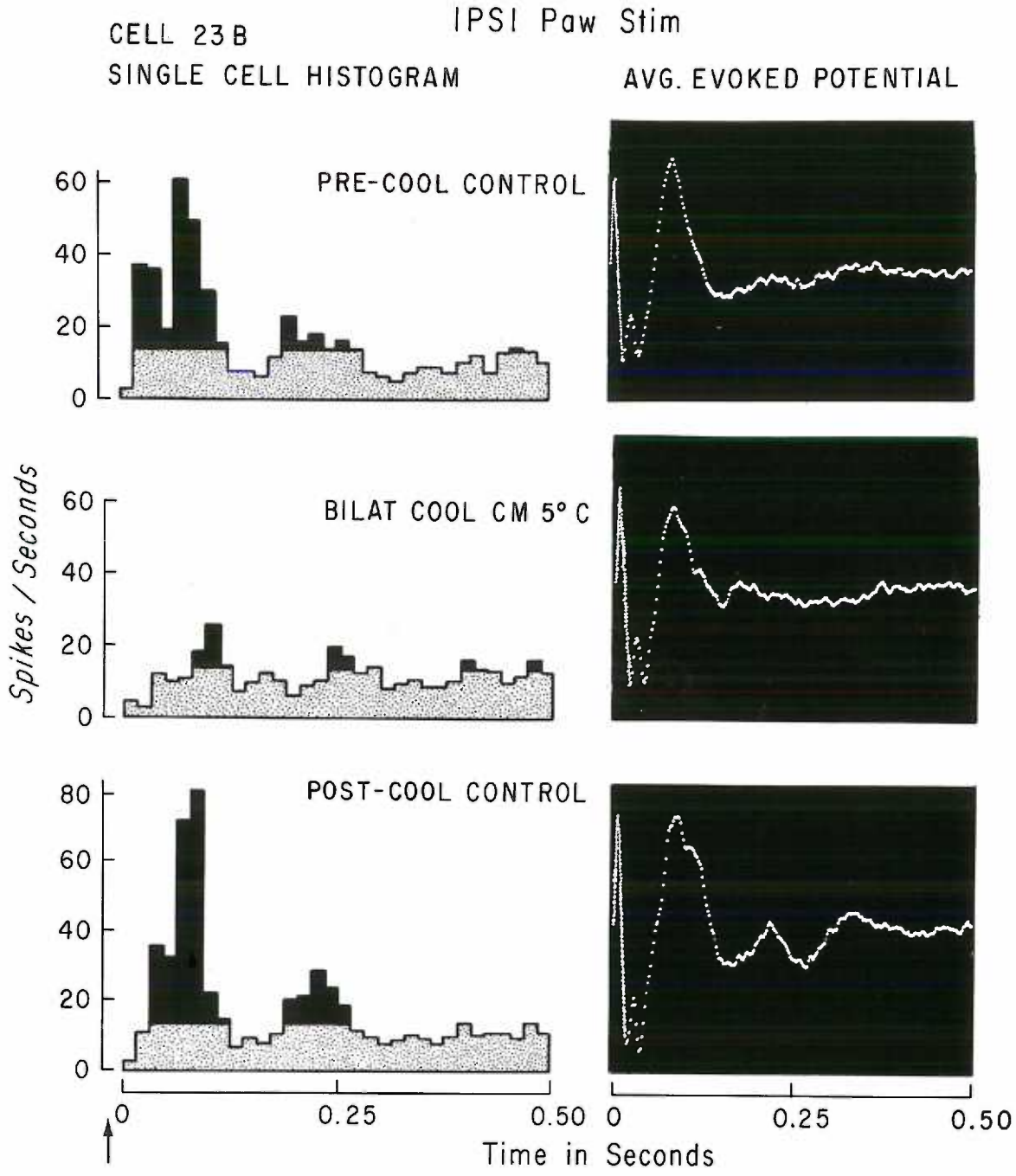
IPSI Paw Stim
CELL 23B
SINGLE CELL HISTOGRAM
AVG. EVOKED POTENTIAL
PRE-COOL CONTROL
BILAT COOL CM 5° C
POST-COOL CONTROL
Spikes / Seconds
60
40
20
0
80
0.25
0.50
Time in Seconds

Figure 6. Summary of unit responses elicited by ipsilateral hindpaw stimulation. The ordinate is the difference score of the post-stimulus spike frequency minus the pre-stimulus spike frequency. Each individual curve represents at least 10 cells.

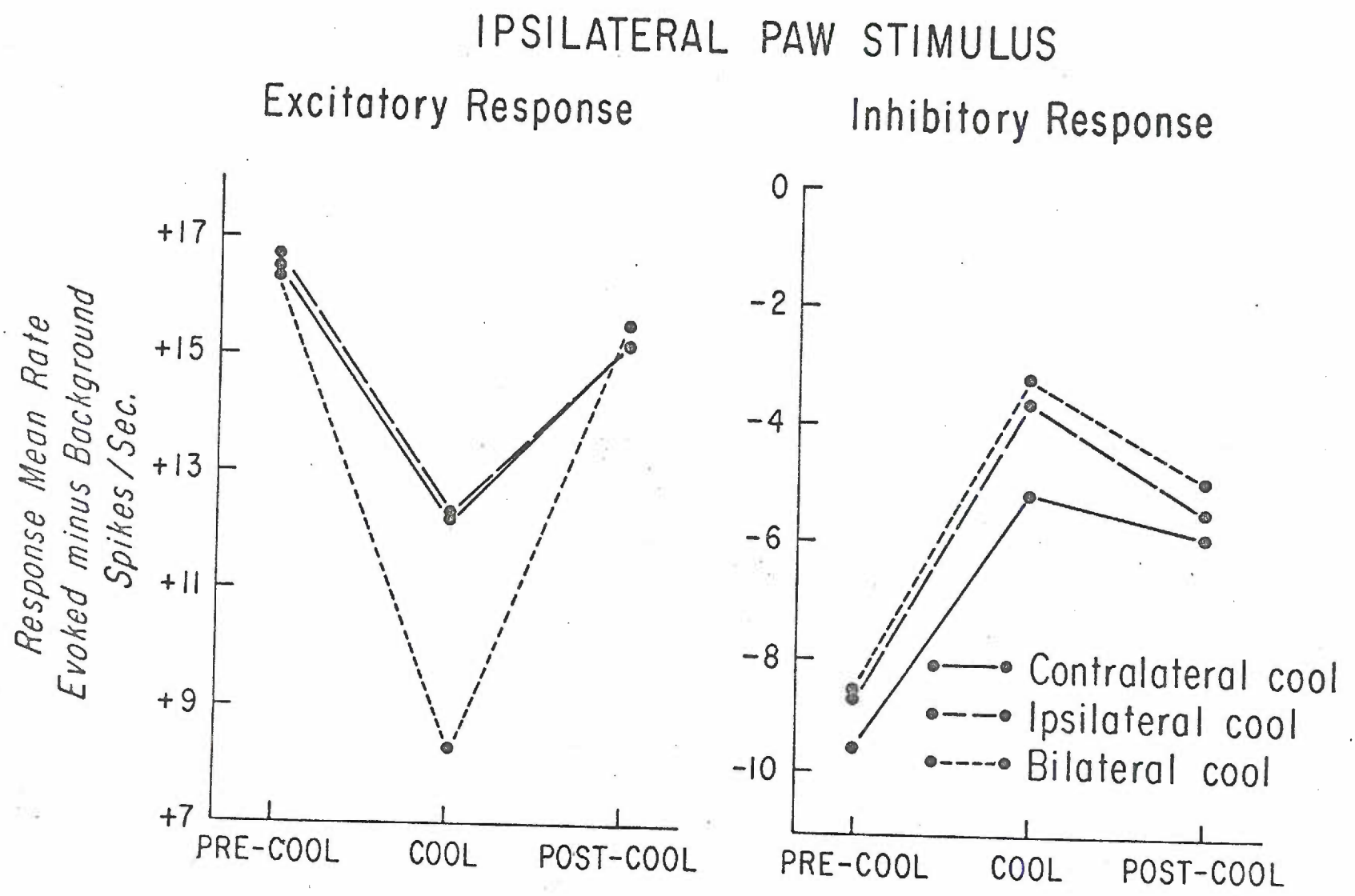
IPSILATERAL PAW STIMULUS
Excitatory Response
Inhibitory Response
Response Mean Rate
Evoked minus Background
Spikes / Sec.
+17
+15
+13
+11
+9
+7
0
-2
-4
-6
-8
-10
PRE-COOL
COOL
POST-COOL
Contralateral cool
Ipsilateral cool
Bilateral cool

elicited by ipsilateral paw stimulation was approximately 16.3 spikes/sec above the background level prior to thalamic cooling. During bilateral thalamic cooling the response rate decreased 49%, to a rate of 8.3 spikes/sec above the background rate. Upon termination of cooling, the response rate increases to about 15.5 spikes/sec above the background rate, approaching the pre-cool value. The grouped data, comprised of 25 neurons, has been evaluated statistically using a t-test for paired data. The decreased rate resulting from bilateral cooling is statistically significant, with a probability of chance occurrence less than .005. The exact mean rates, degrees of freedom, t-values, and significance levels are tabulated in Table 5. Statistical evaluation has been achieved by comparing the pre-cool rate with the cool rate, and by comparing the cool rate with the post-cool rate. The former comparison evaluates the effect of cooling, while the latter measure indexes the extent of recovery subsequent to the termination of cooling.

While bilateral cooling decreased the mean rate by about 8 spikes/sec, either ipsilateral or contralateral thalamic cooling decreased the excitatory response rate by about 4.3 spikes/sec, a reduction of approximately 27% from the initial average response level. The effects from either ipsilateral cooling or contralateral cooling were comparable (Figure 6 cf. solid line with large dashed line). Significant decreases were recorded from the pre-cool to cool response values; similarly, upon termination of cooling, the excitatory response recovers, approaching the pre-cool value. Recovery is significant at the .01 level, in testing the cool with post-cool response rate.

Table 5: Summary of unit responses elicited by ipsilateral hindpaw stimulation

EXCITATORY RESPONSES				INHIBITORY RESPONSES			
Ctrl #1	Bilat Cool		Ctrl. #2	Ctrl #1	Bilat Cool		Ctrl #2
+16.34	+8.27		+15.52	$\bar{X}$ -8.47	-3.19		-4.94
24		24		df 13		13	
4.64		4.09		t 5.00		1.26	
.005		.005		α .005		NS	
Ctrl #1	Ipsi Cool		Ctrl. #2	Ctrl #1	Ipsi Cool		Ctrl #2
+16.67	+12.32		+15.23	$\bar{X}$ -8.66	-3.57		-5.46
23		23		df 10		10	
2.30		3.14		t 4.08		1.15	
.025		.005		α .005		NS	
Ctrl #1	Contra Cool		Ctrl. #2	Ctrl #1	Contra Cool		Ctrl #2
+16.50	+12.24		+15.20	$\bar{X}$ -9.49	-5.24		-5.89
22		22		df 9		9	
2.37		2.59		t 3.65		0.48	
.025		.01		α .005		NS	

The effect of cooling CM on inhibitory response components was to increase the mean spike rate. A grouping of 14 neurons selected for their inhibitory response component showed an average pre-cool response rate of about 8.5 spikes/sec below the pre-stimulus rate. Upon bilateral cooling, this response rate was approximately 3.2 spikes/sec below the pre-stimulus level. The computed t-score shows this increase in mean rate to be significant at the .005 level. Upon termination of bilateral cooling, the difference score became more negative, reflecting a more inhibitory response. The recovery was only partial, being approximately 58% of the initial pre-cooling control.

The greatest decrease in the inhibitory response was achieved in the bilateral cool condition. However, the magnitude of effect was closely paralleled by ipsilateral cooling. Ipsilateral cooling modified the response rate by approximately 5.1 spikes/sec when averaged for 11 neurons. The influence of cooling was significant at the .005 level. Similar to the bilateral cool condition, partial recovery of the inhibitory response was exhibited upon termination of cooling, returning to about 63% of the initial pre-cool control value.

Unilateral cooling, accomplished with the contralateral cooling probe, decreased the inhibitory response, and increased the mean rate. Contralateral cooling was least effective in reducing the inhibitory response, in comparison with either bilateral or ipsilateral cooling. However, contralateral cooling was about 81% as effective as bilateral cooling in its modification of the inhibitory response. Upon termination of cooling, recovery was marginal.

Contralateral paw stimulus

The effect of thalamic cooling on an individual neuron is presented in Figure 7. The unit activity was elicited by stimulation of the contralateral hindpaw. Both the reduction of the excitatory response components (dark) and the inhibitory response components (stippled) are evident during bilateral cooling. It is evident that some portions of the excitatory response are much more influenced during cooling than other portions of the response. In particular, little effect is evident upon the short latency response, while the adjacent portion from about 50 through 100 msec is severely reduced.

The summary of the influence of thalamic cooling on unit responses elicited by contralateral hindpaw stimulation are presented in Figure 8. The data are separated according to response direction, whether excitatory or inhibitory with respect to the pre-stimulus rate. The mean rates, degrees of freedom, t-values, and level of significance are tabulated in Table 6.

The mean rate for the excitatory response derived from 31 cells shows a value of about 29.7 spikes/sec above the pre-stimulus rate during the pre-cool control (Figure 8). Subsequent to bilateral thalamic cooling, the rate decreased to approximately 21.3 spikes/sec, a decrease of about 28%. Upon termination of cooling, the response rate increased toward the initial value, approaching 28 spikes/sec. Both the initial decrease attributed to bilateral cooling and the subsequent recovery were significant at the .005 level.

Partial reductions in the excitatory response were produced by unilateral thalamic cooling. Ipsilateral cooling reduced the response

Figure 7. Post-stimulus histogram of unit activity elicited by contralateral hindpaw stimulation. Mean pre-stimulus rate is represented as stippled area. The excitatory response (darkened) is that which exceeds the pre-stimulus rate. The inhibitory response is evident below the pre-stimulus rate. Stimulus occurrence at arrow. Histogram summed from 100 trials.

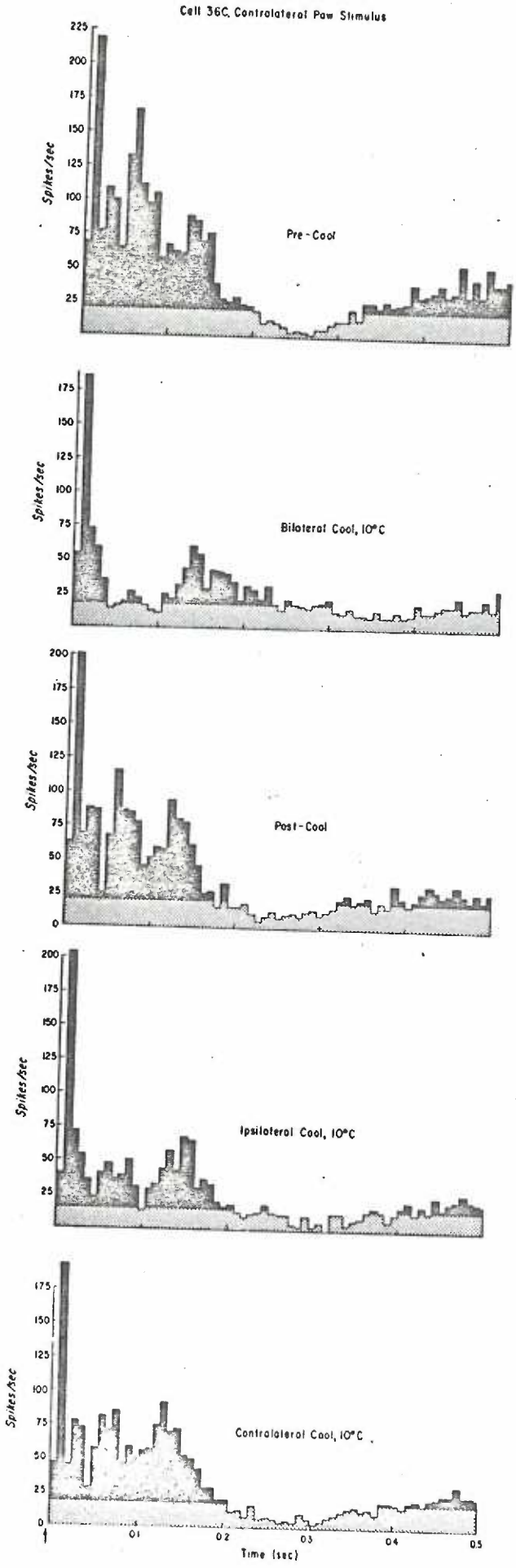
Cell 36C, Contralateral Paw Stimulus
Spikes/sec
Pre-Cool
Bilateral Cool, 10°C
Post-Cool
Ipsilateral Cool, 10°C
Contralateral Cool, 10°C
Time (sec)

Figure 8. Summary of unit responses elicited by contralateral hindpaw stimulation. The ordinate is the difference score of the post-stimulus spike frequency minus the pre-stimulus spike frequency. Each individual curve represents at least 12 cells.

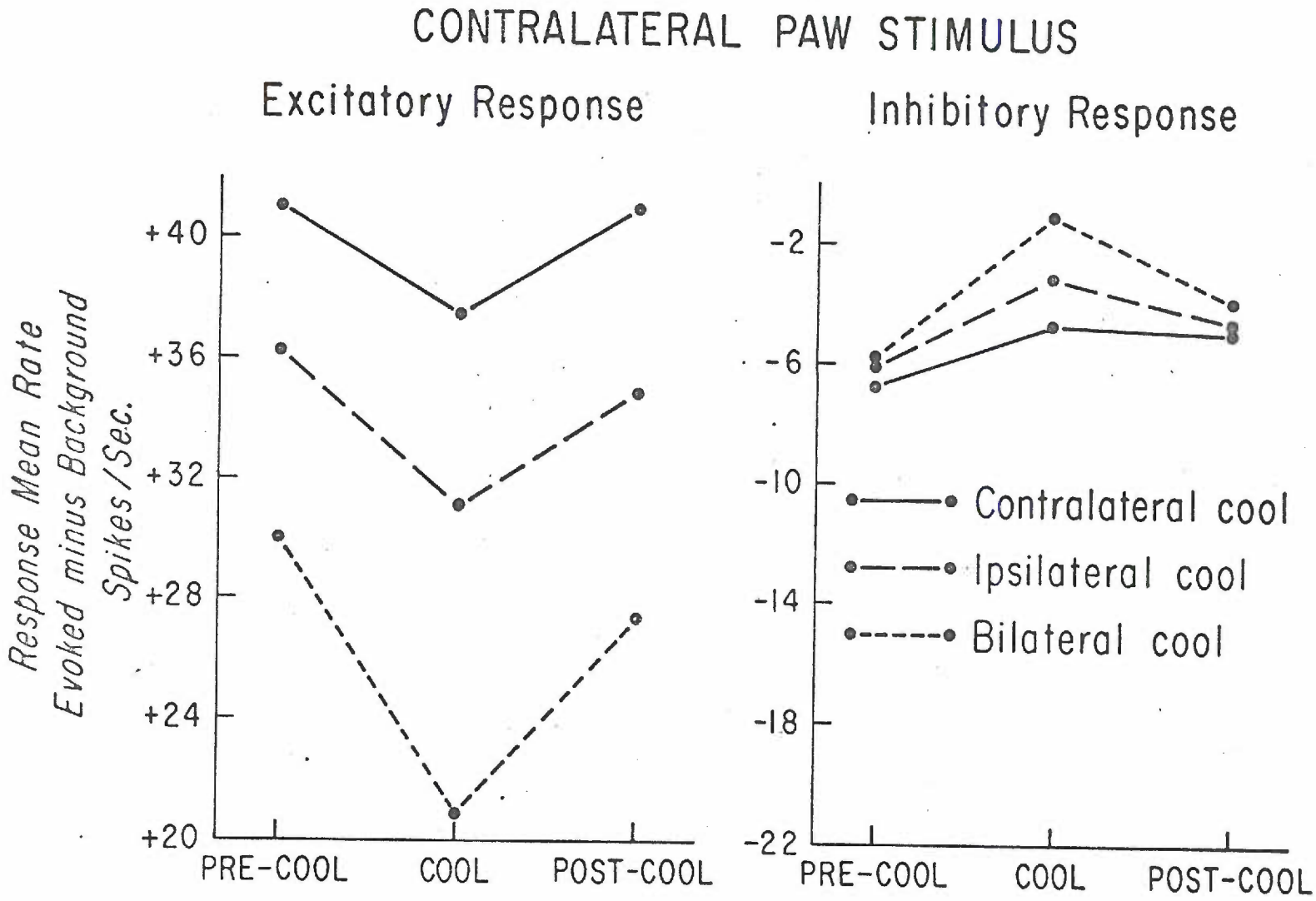
CONTRALATERAL PAW STIMULUS
Excitatory Response
Inhibitory Response
Response Mean Rate
Evoked minus Background
Spikes/Sec.
+40
+36
+32
+28
+24
+20
-2
-6
-10
-14
-18
-22
PRE-COOL
COOL
POST-COOL
PRE-COOL
COOL
POST-COOL
Contralateral cool
Ipsilateral cool
Bilateral cool

Table 6: Summary of unit responses elicited by contralateral hindpaw stimulation

EXCITATORY RESPONSES				INHIBITORY RESPONSES			
Ctrl #1	Bilat Cool	Ctrl #2		Ctrl #1	Bilat Cool	Ctrl #2	
+29.73	+21.27	+27.96	$\bar{X}$	-5.56	-0.95	-3.88	
30	30		df	18	18		
3.72	3.41		t	3.50	2.75		
.005	.005		α	.005	.01		
Ctrl #1	Ipsi Cool	Ctrl #2		Ctrl #1	Ipsi Cool	Ctrl #2	
+36.28	+31.08	+34.93	$\bar{X}$	-5.97	-3.09	-4.52	
21	21		df	11	11		
2.04	2.01		t	2.73	2.53		
.05	.05		α	.01	.025		
Ctrl #1	Contra Cool	Ctrl #2		Ctrl #1	Contra Cool	Ctrl #2	
+41.32	+37.42	+41.05	$\bar{X}$	-6.46	-4.68	-4.88	
17	17		df	13	13		
2.37	2.78		t	2.70	0.41		
.025	.01		α	.01	NS		

rate by 5.2 spikes/sec, being about 62% as effective as bilateral cooling. Contralateral cooling reduced the excitatory response rate from 41.3 spikes/sec to 37.4 spikes/sec, a difference of 3.9 spikes/sec. Contralateral cooling was less than 50% as effective as bilateral cooling in modifying the excitatory response. Both unilateral cooling conditions exhibited significant decreases due to cooling and significant recovery after cooling. The probability of chance occurrence was .05 or less.

The differences in the pre-cooling excitatory response values are due to random sampling differences in the single units that were subjected to the cooling conditions. As a group, those neurons recorded during contralateral thalamic cooling and selected for excitatory response components had a higher initial response rate than the ipsilateral or bilateral cool groups. These chance sampling differences are most evident when examining the excitatory responses elicited by contralateral paw stimulation. However, since each neuron is used in comparing the pre-cool rate with cool and post-cool rate, the sampling deviations are not important.

Similar to the response elicited by ipsilateral hindpaw stimulation, the magnitude of the inhibitory response is smaller than that for the average excitatory response. The initial pre-cool value for the inhibitory responses averages 6 spikes/sec below the baseline, while the initial pre-cool value for the excitatory response averages about 30 spikes/sec above baseline for the bilateral cool group.

The effect of bilateral cooling is to reduce the inhibitory response from 5.6 spikes/sec below baseline to 1.0 spikes/sec below baseline. Partial recovery is evident upon termination of cooling, the inhibitory

response rate returning to 3.9 spikes/sec below baseline. Both the initial decrease in response with incipient cooling and the recovery subsequent to cooling were significant at the .01 level.

Unilateral cooling led to partial modification of the inhibitory response. Ipsilateral cooling decreased the response approximately 63% of that decrease resulting from bilateral cooling, while contralateral cooling resulted in a 39% decrease with respect to that caused by bilateral cooling. The recovery of the response subsequent to the termination of cooling surpassed the .05 level of significance for ipsilateral cooling while recovery from contralateral cooling was marginal.

Light stimulus

The responses elicited by the light stimulus were smallest in magnitude when compared with contralateral and ipsilateral paw stimulation. This generality applied to both excitatory and inhibitory response components. The average pre-cool excitatory response rate was less than 4 spikes/sec above the pre-stimulus rate (Figure 10). The inhibitory response averaged less than 3 spikes/sec below the pre-stimulus rate. However, there was a large range of responsiveness of individual neurons when stimulated with a light flash. For example, included within the grouped data is cell 30 F (Figure 9). Cell 30 F exhibited an instantaneous firing rate of over 72 spikes/sec at about 30 msec post-stimulus. This excitatory response was partially reduced during bilateral thalamic cooling.

The influence of bilateral thalamic cooling was to reduce the excitatory response by an average of 67% (Figure 10). The grouped data for 23 cells showed a decrease from 3.6 spikes/sec to 1.2 spikes/sec.

Figure 9. Post-stimulus histogram of unit activity elicited by light stimulus. Mean pre-stimulus rate is represented as stippled area. The excitatory response is darkened. Stimulus occurrence at arrow. Histogram summed from 100 trials.

CELL 30F, LIGHT STIMULUS

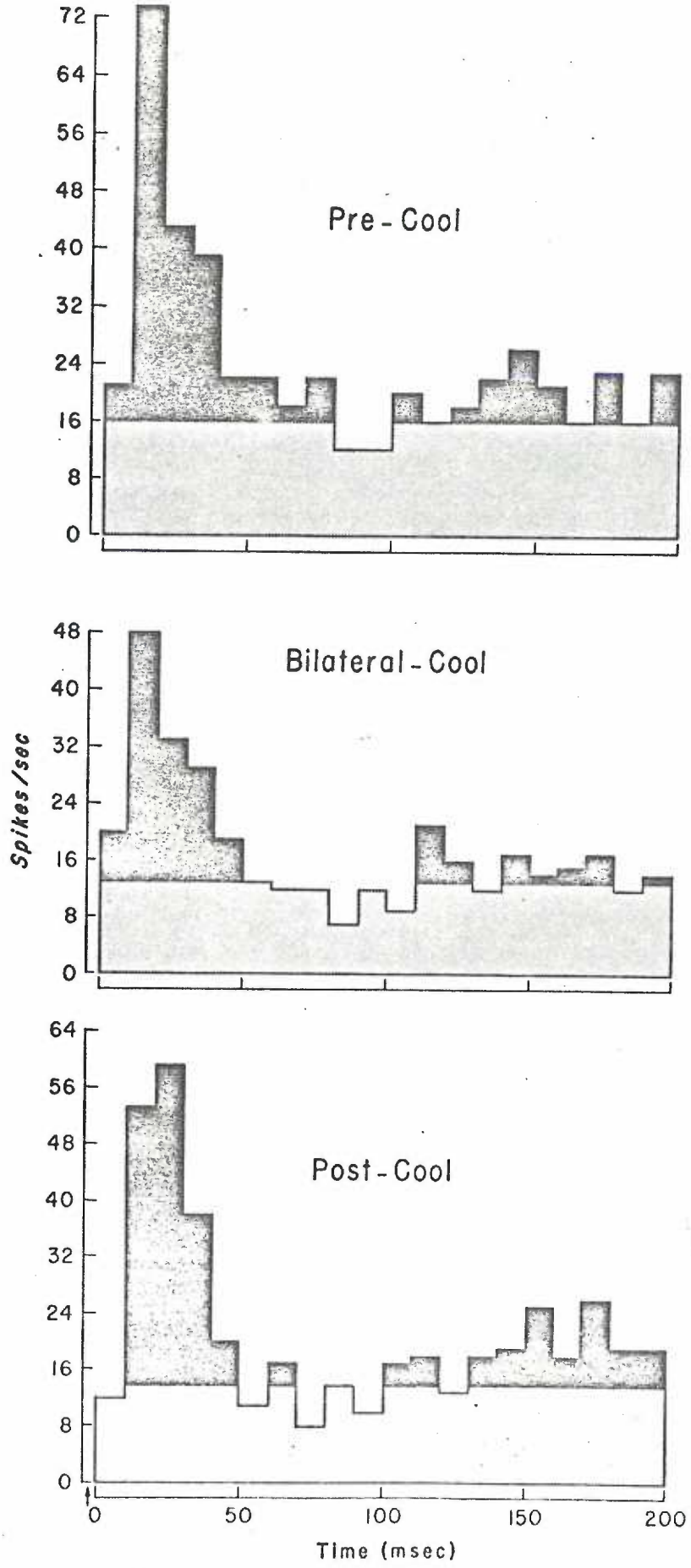

Figure 10. Summary of unit responses elicited by light stimulus. The ordinate is the difference score of the post-stimulus spike frequency minus the pre-stimulus spike frequency. Each individual curve represents at least 11 cells.

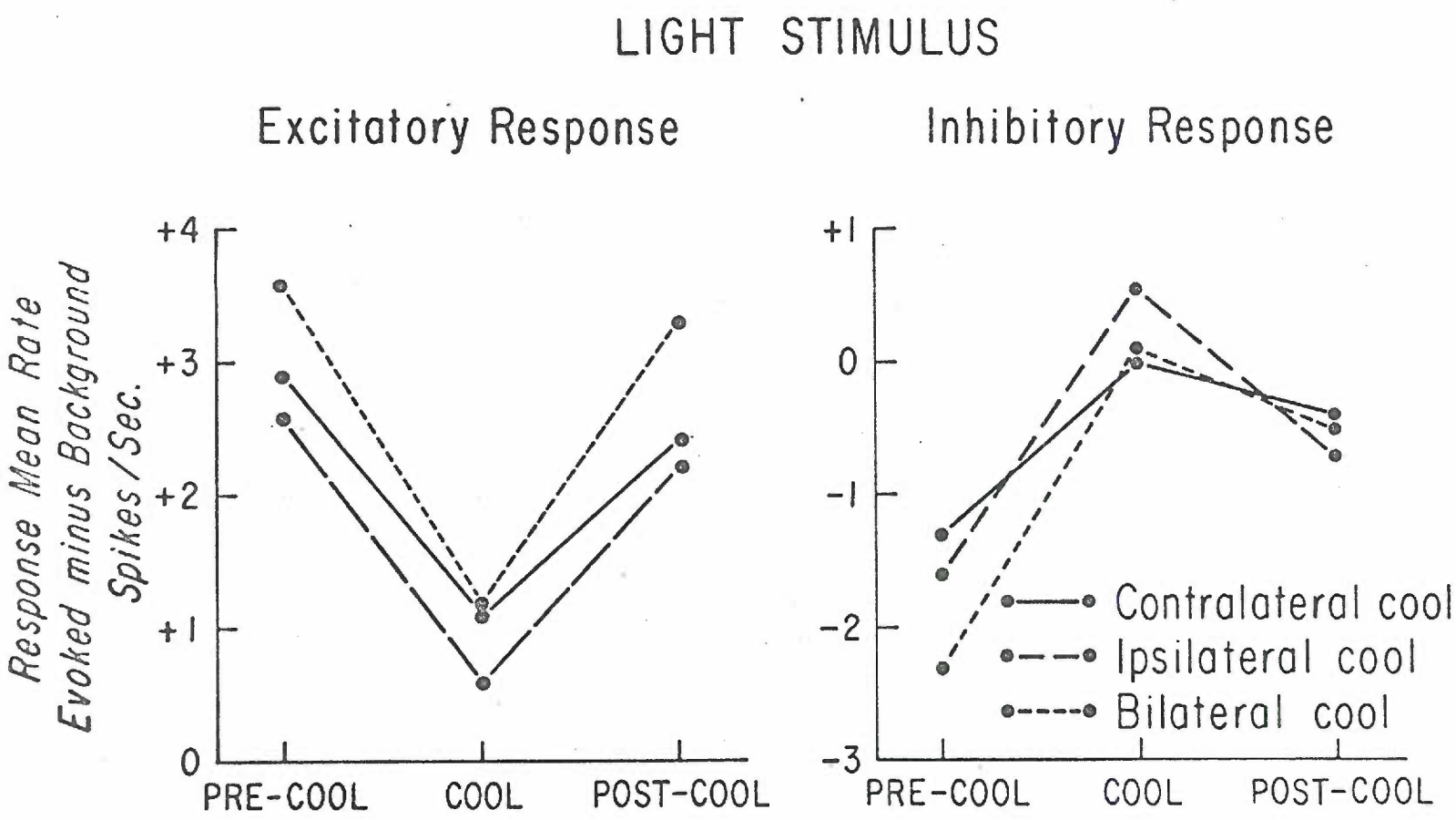
LIGHT STIMULUS
Excitatory Response
Inhibitory Response
Response Mean Rate
Evoked minus Background
Spikes / Sec.
+4
+3
+2
+1
0
+1
0
-1
-2
-3
PRE-COOL
COOL
POST-COOL
PRE-COOL
COOL
POST-COOL
Contralateral cool
Ipsilateral cool
Bilateral cool

Upon termination of cooling, the excitatory response recovered, approaching 3.3 spikes/sec. Both the initial decrease caused by cooling and the recovery were significant at the .005 level.

Unilateral cooling resulted in decreases in the excitatory responses elicited by the light, although neither ipsilateral nor contralateral cooling were as effective as bilateral cooling. Ipsilateral cooling was about 83% as effective as bilateral cooling, while contralateral cooling was the least effective in reducing the unit response.

The effect of cooling on the inhibitory response was to increase the mean spike rate, thus tending to bring the response toward the baseline. Significant increases in firing rate were seen for all three modes of cooling. Bilateral cooling was most effective and modified the average response from 2.4 spikes/sec below baseline to 0.2 spikes/sec above baseline, an elimination of the inhibitory response. Upon termination of cooling, the response recovered its inhibitory characteristic.

In a similar manner, unilateral cooling yielded an increase in response firing rate during the average inhibitory response. Ipsilateral cooling brought the response from below baseline to 0.6 spikes/sec above the baseline level. Again, contralateral cooling abolished the inhibitory response, bringing the firing rate to the baseline. The recovery in each case was partial, but sufficient for the response to return to its inhibitory characteristic. The mean values, degrees of freedom, t-scores, and levels of significance are tabulated in Table 7.

Table 7: Summary of unit responses elicited by light stimulus

	EXCITATORY RESPONSES			INHIBITORY RESPONSES		
	Ctrl #1	Bilat Cool	Ctrl #2	Ctrl #1	Bilat Cool	Ctrl #2
$\bar{X}$	+3.60	+1.18	+3.33	-2.39	+0.15	-0.45
df	22	22		21	21	
t	3.53	3.91		4.00	0.65	
α	.005	.005		.005	NS	
	Ctrl #1	Ipsi Cool	Ctrl #2	Ctrl #1	Ipsi Cool	Ctrl #2
$\bar{X}$	+2.57	+0.61	+2.24	-1.66	+0.55	-0.70
df	14	14		10	10	
t	2.87	2.55		3.66	1.41	
α	.01	.025		.005	NS	
	Ctrl #1	Contra Cool	Ctrl #2	Ctrl #1	Contra Cool	Ctrl #2
$\bar{X}$	+2.87	+1.11	+2.44	-1.32	+0.02	-0.39
df	10	10		12	12	
t	1.70	1.85		2.22	0.46	
α	NS	.05		.025	NS	

Evoked potential results

The evoked potential data were separated according to stimulus and analyzed both for peak-to-peak amplitude and for the integral of the waveform. The results can best be understood from the summary of the grouped data.

Ipsilateral paw stimulation

Ipsilateral hindpaw stimulation gave rise to a complex waveform as recorded from the postcruciate cortex (Figure 5, right column). Since the amplification gain was constant during the recording of any one cell, it was possible to compare the evoked potential summed from 100 trials prior to cooling, with that of the cool condition and the post-cool control. A substantial decrease is evidenced in the peak-to-peak amplitude of the secondary components of the AEP, occurring at about 100 msec after stimulus onset. Upon termination of cooling, the amplitude of the waveform increases, in this case exceeding the initial pre-cool value. Some variability of waveform is evidenced in the longer latency fluctuations.

The techniques used for peak-to-peak and integral analysis have been described previously (see Methods). Figure 11 depicts an ipsilateral paw stimulus AEP which was rectified and integrated. The area analysis was derived from the ordinate value of the integrated AEP at 0.5 sec post-stimulus. The peak-to-peak analysis was done by placing cursors on the peak positive and negative deflections and obtaining the quantitative difference in peak-to-peak amplitude. For the AEPs evoked by ipsilateral paw stimulation, the shorter latency peak had a mean latency of 29 msec with a standard deviation of 17 msec, while

Figure 11. Area and interval analysis of evoked potentials. The left column depicts area analysis of the pre-cool condition. The averaged evoked potential was summed over 100 presentations of ipsilateral paw stimulus (upper left). The AEP was rectified by using absolute values of difference from baseline (middle left). The cummulative values of the rectified AEP are summed to give the area under the curve (lower left). The sequence yielding area under the curve is depicted for the bilateral cool condition in the middle column. Using the integrated AEPs, the interval most affected by cooling was determined (right column). The pre-cool integrated AEP was positioned over the bilateral cool integrated AEP (upper right). The initial portion superimposes and the left cursor was set at the point of divergence. The bilateral cool trace was then positioned over the pre-cool trace with the right cursor set at the resumption of convergence (middle right). The interval defined by the cursors is that segment most affected by cooling. The selected interval recovers after termination of cooling, as evidenced by a comparison of the pre-cool trace with the post-cool trace (lower right).

AREA and INTERVAL ANALYSIS
Cat 39A, Ipsilateral Paw Stimulus

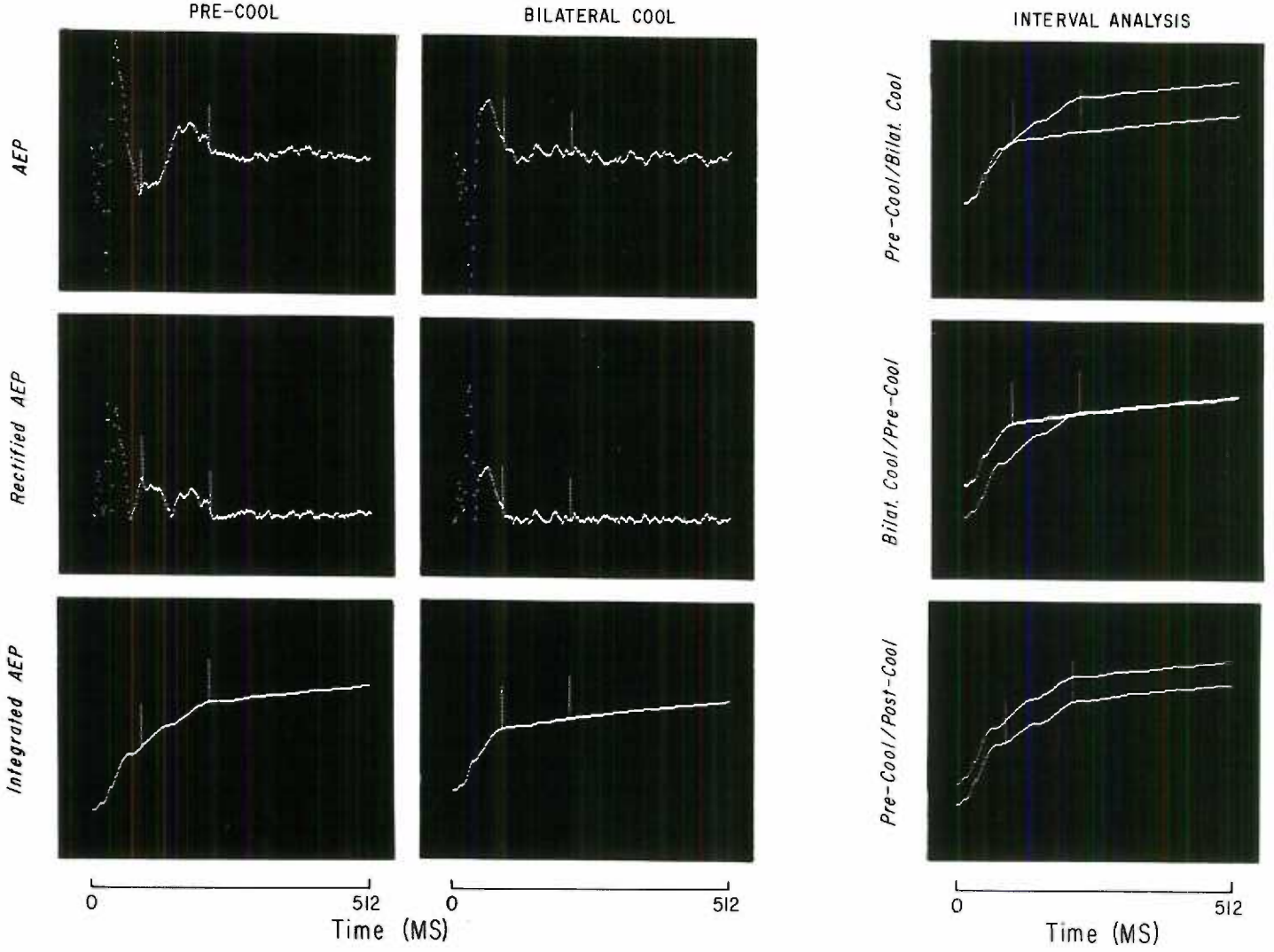

the longer latency peak had a mean latency of 50 msec with a standard deviation of 25 msec. Figure 12 contains the grouped data analyzed according to the two different methods. In general, the results obtained through the peak-to-peak measure corresponded with the results of the integral analysis. It should be evident that the peak-to-peak amplitude analysis measures a restricted temporal portion of the AEP. The difference between peak and trough in the peak-to-peak measurement might approximate 20 msec. In contrast, the integral analysis, analysis of the area under the EP waveform, is more expansive temporally. The area analysis includes approximately 0.5 sec of EP waveform, or about 25 times the time base included in the peak-to-peak analysis. The results indicate that both the peak-to-peak analysis and area analysis are sensitive to the changes in the AEP caused by thalamic cooling, with a greater magnitude of change revealed in the peak-to-peak measure.

As shown in Figure 12, bilateral cooling of CM region decreased the peak-to-peak amplitude over 50% when compared with the pre-cool control value. The data comprised the evoked potentials associated with 41 single cell recordings. The post-cool control exhibited virtually complete recovery, being within 1.5% of the initial control. Both the decrease in amplitude, resulting from cooling, and the recovery after cooling were highly significant. Table 8 contains the average percentage decrease, the degrees of freedom, t-value, and level of significance for a paired t-test.

Both ipsilateral and contralateral cooling were effective in the partial decrease of the EP amplitude. Ipsilateral cooling yielded a

Figure 12. Summary of averaged evoked potentials from ipsilateral hindpaw stimulation. "N" equals the number of averaged evoked potentials contributing to each point plotted. The ordinate is the average percent decrease of the AEPs with respect to the pre-cool control.

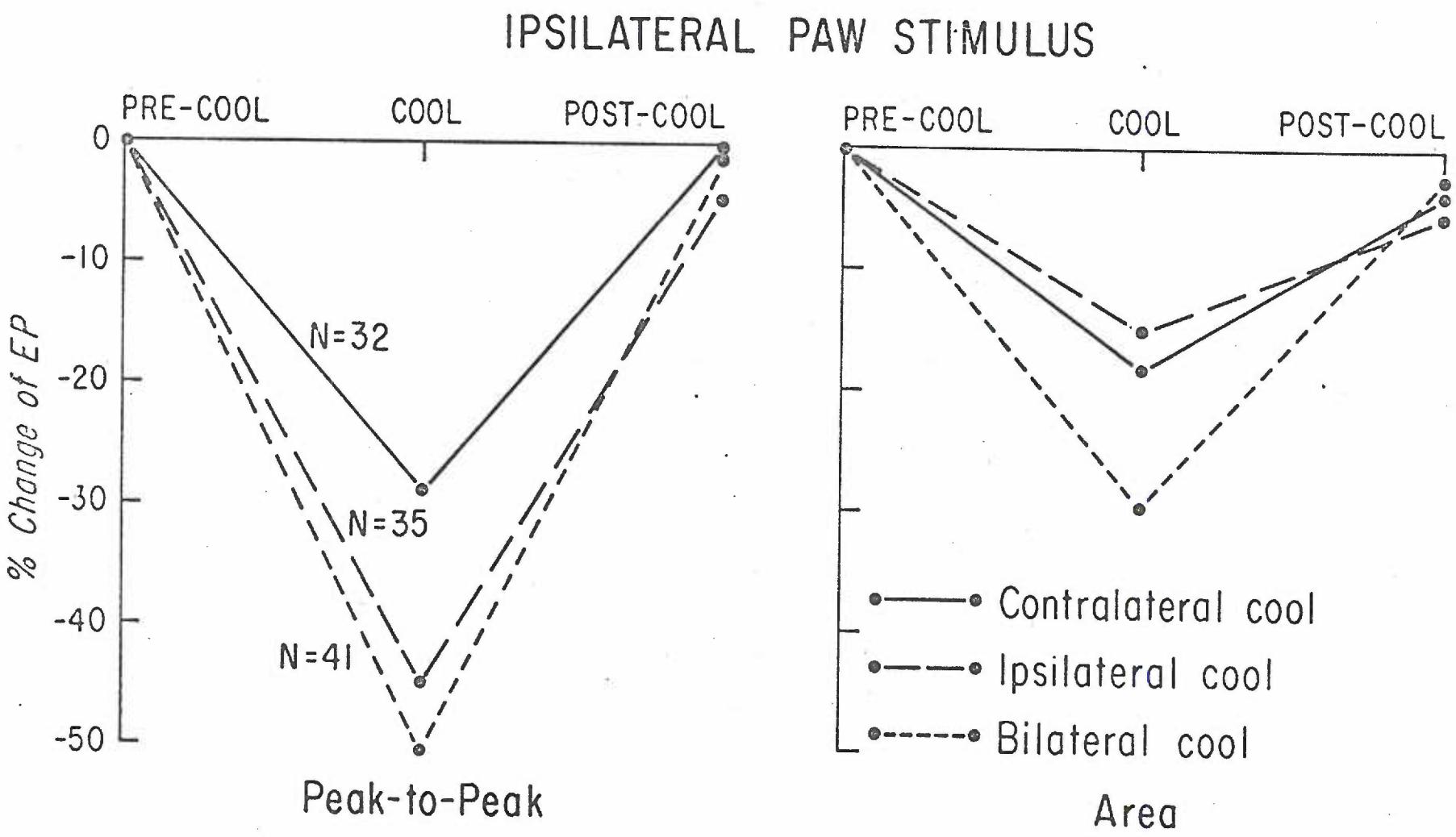
IPSILATERAL PAW STIMULUS
PRE-COOL
COOL
POST-COOL
0
-10
-20
-30
-40
-50
% Change of EP
N=32
N=35
N=41
Peak-to-Peak
PRE-COOL
COOL
POST-COOL
Contralateral cool
Ipsilateral cool
Bilateral cool
Area

Table 8: Ipsilateral paw stimulus evoked potentials

% Change of AEP	PEAK-TO-PEAK		AREA	
	Bilat Cool -50.8	Post-Cool -1.34	Bilat Cool -29.73	Post-Cool -2.56
	df 40, t = 12.58, p < .005		df 40, t = 7.54, p < .005	
	Ipsi Cool -44.79	Post-Cool -4.90	Ipsi Cool -15.26	Post-Cool -6.53
	df 34, t = 7.56, p < .005		df 33, t = 1.77, p .05	
	Contra Cool -28.88	Post-Cool -0.59	Contra Cool -18.16	Post-Cool -3.72
	df 31, t = 5.77, p < .005		df 31, t = 4.58, p < .005	

45% decrement of amplitude, while contralateral cooling resulted in a 29% decrease. In both cases excellent recovery is exhibited, the difference between the experimental and control conditions being highly significant.

A similar pattern is evident from the area analysis. The area measure is less dramatic, the changes being about one-half the magnitude of the peak-to-peak modifications. Bilateral cooling decreased the area under the evoked potential an average of 29.7%. Upon termination of cooling, the integral recovered to within 2.6% of the initial value, which was statistically significant. Unilateral cooling was less effective than bilateral cooling in yielding decreases. Contralateral cool resulted in an 18.2% decrease, while ipsilateral cooling decreased the integral by 15.3%. Again, recovery was evident subsequent to terminating cooling.

Contralateral paw stimulation

The pattern of effect of thalamic cooling on the evoked potentials elicited by contralateral paw stimuli is comparable with that described for ipsilateral paw stimulation. An example of an evoked potential averaged for 100 stimulus presentations is shown in Figure 3 (right column). The most obvious change resulting from cooling appears in the longer latency fluctuations, which appear to be abolished. The secondary components are diminished in size, while the primary component is relatively unaffected.

The extent of the decrease of the evoked potential has been quantified for the grouped data, using both the peak-to-peak measure and the area measure. The effect of bilateral thalamic cooling is a

substantial reduction in the evoked potential (Figure 13). The peak-to-peak measure showed an average decrease of 45% with respect to the pre-cool control amplitude. For the peak-to-peak measure of the AEPs elicited by contralateral paw stimulation, the shorter latency peak had a mean latency of 35 msec with a standard deviation of 19 msec, while the longer latency peak had a mean latency of 62 msec with a standard deviation of 28 msec. The area measure, extending over the 0.5 sec duration of the evoked potential, showed a 20% average decrease. A paired t-test showed that the recovery, subsequent to the termination of cooling, was highly significant for both the peak-to-peak and area measures (Table 9).

Results further indicated that a reliable decrement in the evoked potential resulted from unilateral thalamic cooling. Ipsilateral cooling yielded consistently greater decreases, which averaged 34% for the amplitude decrease and 10% for the area reduction. Although recovery is not complete, the differences between the cool conditions and the post-cool controls are statistically significant.

The least dramatic changes are evidenced from contralateral cooling. The peak-to-peak amplitude is diminished almost 20%. Partial recovery is evident after rewarming. Contralateral cooling decreases the evoked potential area about 6% from the initial pre-cool value, returning within 1.5% of the initial value after cooling. The average values, degrees of freedom, paired t-values, and levels of significance are contained in Table 9.

Figure 13. Summary of averaged evoked potentials from contralateral paw stimulation. "N" equals the number of averaged evoked potentials contributing to each point plotted. The ordinate is the average percent decrease of the AEPs with respect to the pre-cool control.

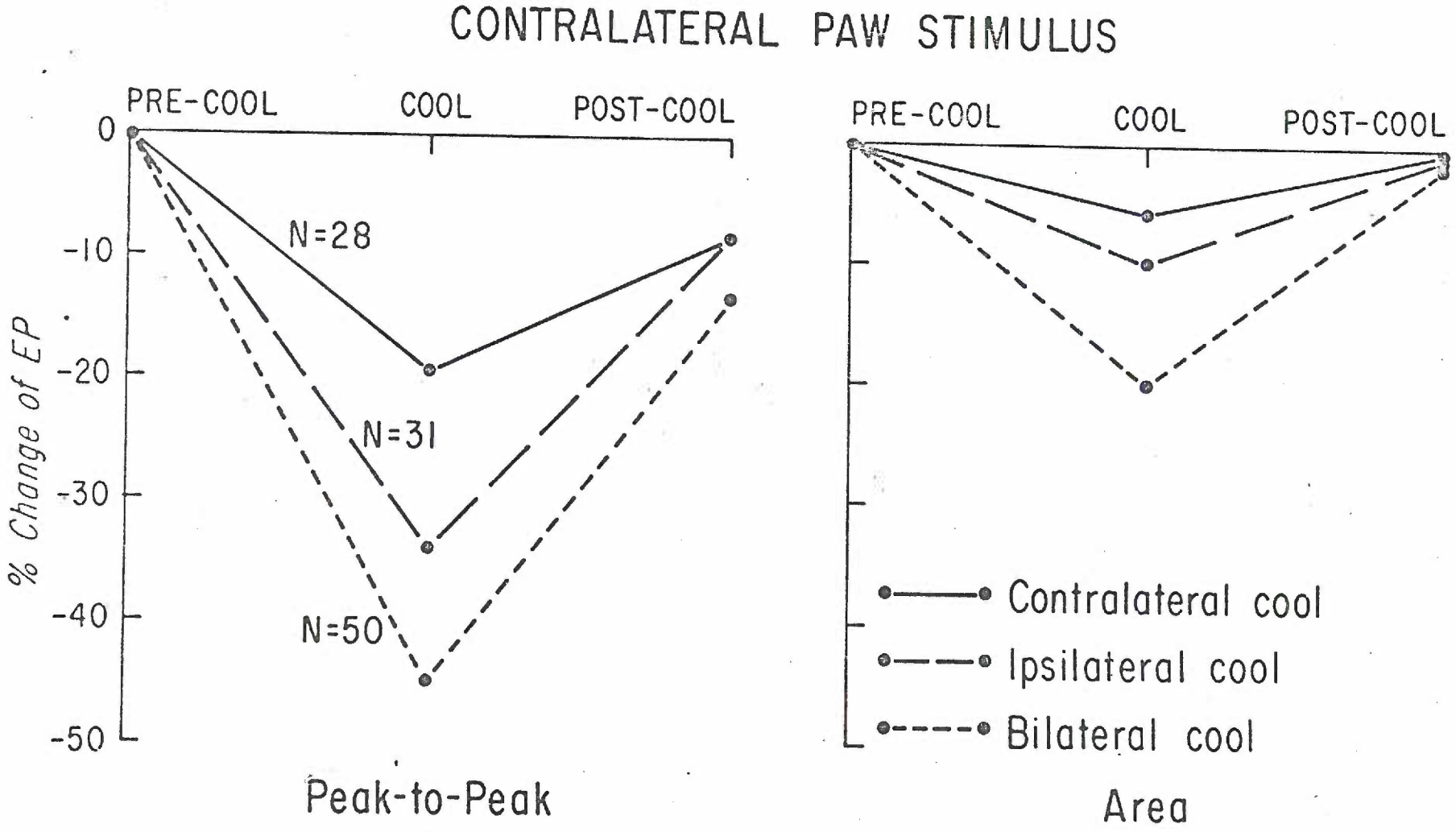
CONTRALATERAL PAW STIMULUS
PRE-COOL
COOL
POST-COOL
0
-10
-20
-30
-40
-50
% Change of EP
N=28
N=31
N=50
Peak-to-Peak
PRE-COOL
COOL
POST-COOL
Contralateral cool
Ipsilateral cool
Bilateral cool
Area

Table 9: Contralateral paw stimulus evoked potentials

% Change of AEP	PEAK-TO-PEAK			AREA		
	Bilat Cool		Post-Cool	Bilat Cool		Post-Cool
	-45.08		-13.20	-20.17		-2.33
		df 49 t = 9.03 p < .005			df 51 t = 6.30 p < .005	
	Ipsi Cool		Post-Cool	Ipsi Cool		Post-Cool
	-33.97		-8.42	-9.88		-1.67
		df 30 t = 7.42 p < .005			df 32 t = 3.44 p < .005	
	Contra Cool		Post-Cool	Contra Cool		Post-Cool
	-19.61		-8.71	-6.03		-1.55
		df 27 t = 2.58 p < .01			df 30 t = 1.27 p = N.S.	

Evoked potential data: Light stimulus

The effect of thalamic cooling on the light evoked potentials differed from that of the paw stimuli. In contrast, a substantial proportion of the light elicited evoked potentials increased in amplitude and area during thalamic cooling. In fact, 24% of the recorded evoked potentials increased in peak-to-peak amplitude during bilateral cooling. Consequently it was deemed advantageous to distinguish two groups for the light stimulus evoked potential data: (1) those for which cooling enhanced the evoked potentials and (2) those decremented by cooling (Figure 14).

The predominant effect of bilateral thalamic cooling was to reduce the light stimulus evoked potentials. For this group, significant decreases in the evoked potentials resulted from any cooling, whether bilateral or unilateral. Excellent recovery is evidenced upon termination of cooling. Bilateral cooling is most effectual, both in the peak-to-peak decrement and the area reduction, with average decreases of 40% and 18% recorded respectively. Unilateral cooling is almost as effective as bilateral cooling which is most evident in the near coincidence of the cooling values for the decrease in area (Figure 14, lower right graph). Ipsilateral cooling, resulting in a 36% decrease in amplitude, closely approximates the bilateral cool condition decrement (Figure 14, lower left).

A smaller number of evoked potentials were enhanced during the cooling conditions. For 12 evoked potentials, bilateral cooling yielded a 36% increase in amplitude. Contralateral and ipsilateral cooling resulted in respective increases of 21% and 16%. Only partial recovery is evidenced subsequent of thalamic rewarming (Table 10).

Figure 14. Summary of the averaged evoked potentials from light stimulus. Two groups exist for the light data; those for which cooling enhanced the averaged evoked potentials (upper graphs), and those which were decreased with cooling (lower graphs). The ordinate corresponds to the average percent increase or decrease of the AEPs with respect to the pre-cool control. "N" equals the number of averaged evoked potentials contributing to each point plotted.

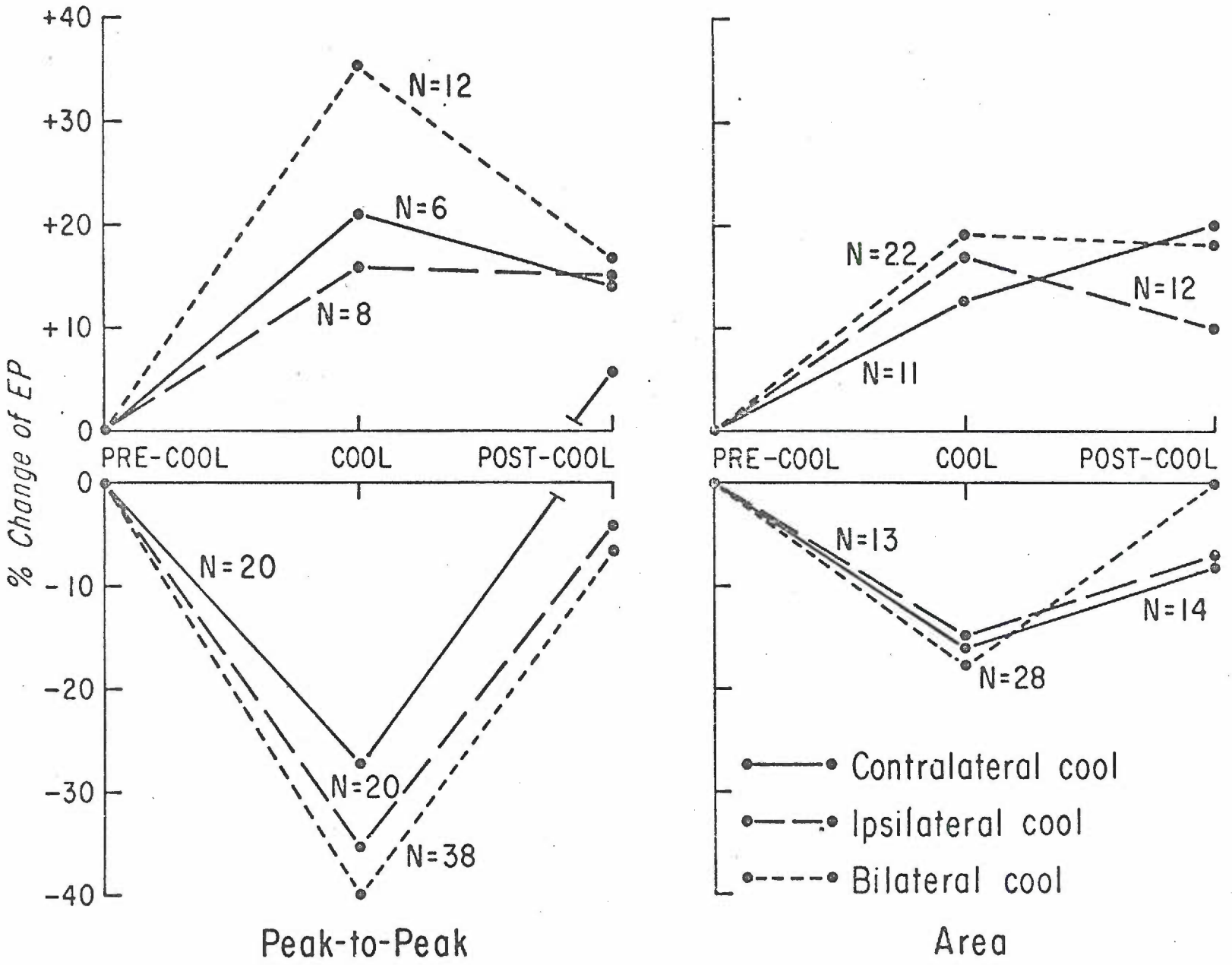
LIGHT STIMULUS
+40
+30
+20
+10
0
-10
-20
-30
-40
% Change of EP
N=12
N=6
N=8
N=20
N=20
N=38
PRE-COOL
COOL
POST-COOL
Peak-to-Peak
N=22
N=12
N=11
N=13
N=14
N=28
Contralateral cool
Ipsilateral cool
Bilateral cool
Area

Table 10: Light stimulus evoked potentials

% Change of AEP	PEAK-TO-PEAK			AREA		
Enhancement	Bilat Cool +35.9	df 11 t = 1.3 p = N.S.	Post-Cool +17.3	Bilat Cool +18.85	df 21 t = 0.0 p = N.S.	Post-Cool +18.58
	Ipsi Cool +15.62	df 7 t = 0.0 p = N.S.	Post-Cool +15.63	Ipsi Cool +17.42	df 11 t = 1.14 p = N.S.	Post-Cool +9.83
	Contra Cool +21.0	df 5 t = 0.9 p = N.S.	Post-Cool +13.8	Contra Cool +12.73	df 10 t = 1.18 p = N.S.	Post-Cool +20.36
Decrement	Bilat Cool -40.1	df 37 t = 3.97 p < .005	Post-Cool -6.9	Bilat Cool -17.68	df 27 t = 5.47 p < .005	Post-Cool 0.0
	Ipsi Cool -36.1	df 19 t = 3.27 p < .005	Post-Cool -3.95	Ipsi Cool -15.08	df 12 t = 1.48 p = N.S.	Post-Cool -7.08
	Contra Cool -27.65	df 19 t = 3.94 p < .005	Post-Cool +6.05	Contra Cool -16.79	df 13 t = 1.97 p < .05	Post-Cool -8.79

A similar pattern is shown by the area analysis. Less than half of the light stimulus evoked potentials were enhanced by thalamic cooling. Twenty-two EP recordings showed an average enhancement of 19%. Unilateral cooling similarly resulted in increased area of some light stimulus evoked potentials. Either ipsilateral or contralateral cooling was less effective than bilateral cooling. Only partial recovery, if any, was observed subsequent to cooling termination. Further distinction between the light enhancement and decrement effects was seen through the interval analysis.

Interval analysis

The evoked potential area measure was found to be a useful index of the interval of the response most affected by the cooling blockade. Figure 11 illustrates the process by which the interval analysis was accomplished. It was possible to superimpose the curves describing the EP area. Initially the pre-cool control curve was compared with the bilateral cool curve. The initial portion of the responses appeared identical and could be superimposed. Using a cursor, the point of divergence was noted. The bilateral cool trace was then positioned over the latter portion of the pre-cool control curve. Again, a cursor was placed at the resumption of convergence. Figure 11 illustrates the typical situation. There are two portions of the integrated AEPs which can be virtually superimposed, with an aberrant portion between the two. The interval analysis allowed an identification of the aberrant portion which was described with reference to the time post-stimulus.

In some cases the aberrant portion was best described as two intervals within three superimposed portions. The interval analysis was on occasion quite fine grained, the critical interval being only 12 msec. The largest interval recorded was 240 msec. However, most of the intervals were between 50 through 100 msec in duration. For this analysis, the comparison was made between the pre-cool control and bilateral cool, omitting all unilateral cooling conditions. By summing these aberrant portions, a histogram of the intervals influenced by bilateral cooling was derived (Figure 15). The histograms describe the number of evoked potentials affected at any specified time after the stimulus, and were formulated for each stimulus. A median was computed to describe the central tendency of each histogram, since the median is the measure of choice for describing skewed distributions. Variation from the median has been described as plus and minus one quartile.

A histogram for the ipsilateral paw stimulus is shown in the upper graph of Figure 15. This histogram reflects the particular portion of the AEP most affected by bilateral thalamic cooling. The median is 142 msec. One quartile on each side of the median has been shaded, and thus the darkened area describes 50% of the response intervals affected by cooling. The first quartile falls at 98 msec, the third quartile falls at 193 msec, and 28 AEP pairs were used to derive the histogram. It should be noted that very few response intervals were affected within 40 msec post-stimulus nor were many intervals described beyond 240 msec post-stimulus. There was no evidence for cooling effects on the response beyond 380 msec extending through 500 msec post-stimulus.

Figure 15. Response interval affected by bilateral cooling. The histograms represent the percentage of averaged evoked potentials affected at any specified time after the stimulus. The median is shown for each histogram with $\pm$ 1 quartile shaded dark gray. The light stimulus histogram is broken into those AEPs enhanced by cooling and those diminished by cooling.

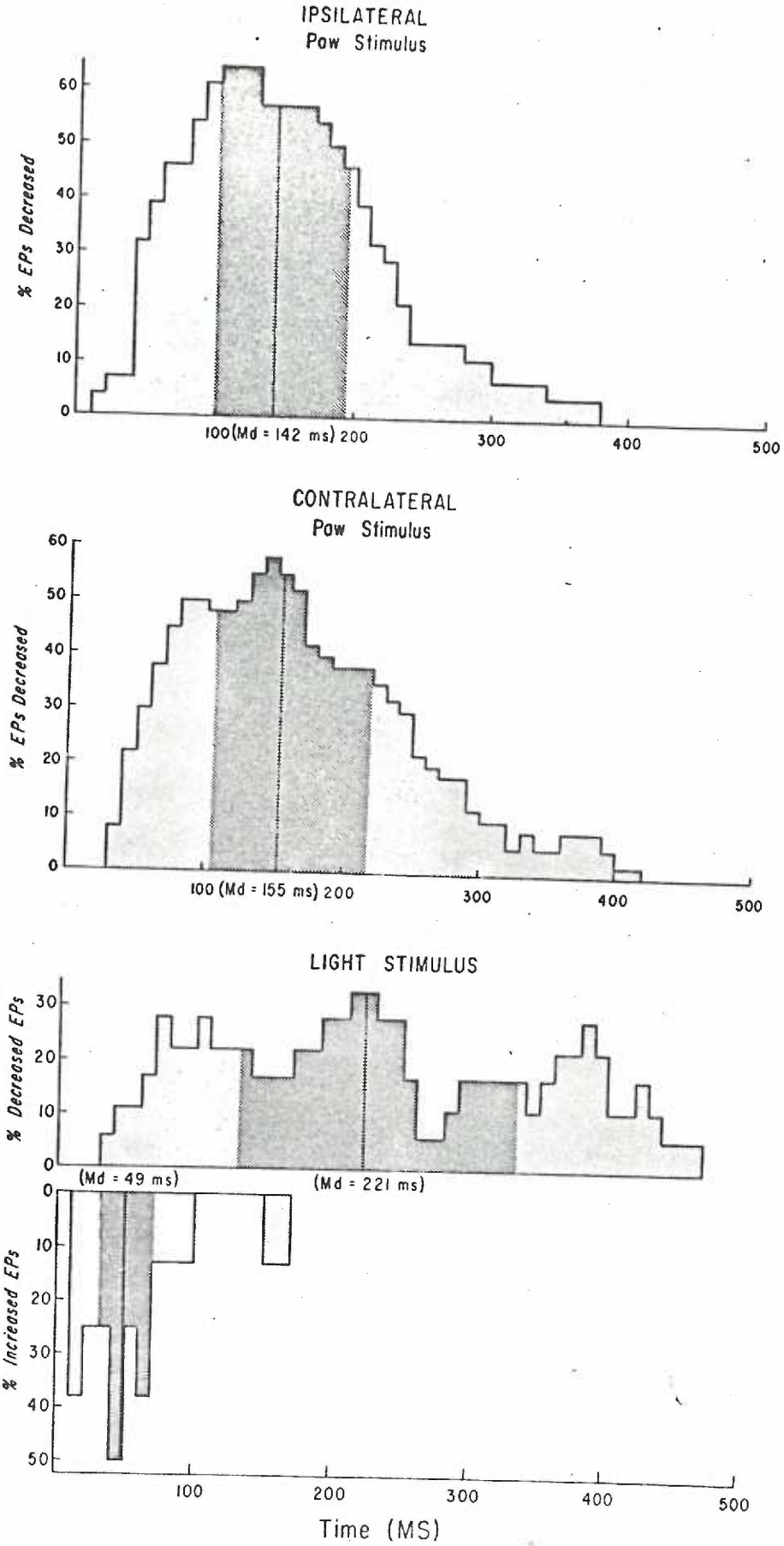
IPSILATERAL
Paw Stimulus
% EPs Decreased
60
50
40
30
20
10
0
100(Md = 142 ms) 200
300
400
500
CONTRALATERAL
Paw Stimulus
% EPs Decreased
60
50
40
30
20
10
0
100 (Md = 155 ms) 200
300
400
500
LIGHT STIMULUS
% Decreased EPs
30
20
10
0
(Md = 49 ms)
(Md = 221 ms)
% Increased EPs
0
10
20
30
40
50
100
200
300
400
500
Time (MS)

A similar histogram has been derived for the contralateral paw stimulus (Figure 15, middle graph). The median lies at 155 msec, with plus and minus 1 quartile shaded. The first quartile value is 105 msec, the third quartile value is 218 msec, and 40 AEP pairs were used in computing the histogram. The shape and distribution of the contralateral paw response intervals affected by cooling is comparable with that derived for ipsilateral paw stimulation. None of the response prior to 30 msec post-stimulus appears to be influenced by bilateral thalamic cooling. As in the case with ipsilateral paw stimulation, most of the effect of bilateral cooling is evidenced between 100 through 200 msec post-stimulus.

The distribution of light response intervals affected by bilateral cooling is in contrast with that for both somatic stimuli (Figure 15). Unlike the somatic stimuli, bilateral cooling often enhanced the AEP elicited by the light stimulus. Consequently two histograms were derived; one for the AEPs decreased during bilateral cooling, and a second for those AEPs increased during bilateral thalamic cooling.

The histogram for AEPs decreased by cooling shows a diffuse distribution of affected intervals. The median is at 221 msec. The variability is evidenced by the spread of plus and minus 1 quartile, extending from 135 msec through 333 msec for the third quartile. The distribution appears to be trimodal rather than unimodal. Responses less than 30 msec were not influenced by bilateral cooling. However, in contrast with the somatic stimuli, cooling affected the light elicited responses during the later portions of the response, extending through the limit of data collection, 0.5 sec.

The histogram for AEPs enhanced by bilateral thalamic cooling shows a distribution confined within the period shortly after the stimulus. The median for the enhancement effect is 49 msec post-stimulus. The first quartile value is 30 msec and the third quartile value is 70 msec, thus 75% of the EP enhancement during cooling occurs prior to 70 msec post-stimulus, the third quartile. There is only a slight overlap with the light stimulus decrement group (cf. upper and lower histograms, light stimulus). The enhancement distribution appears to be unimodal. No enhancement effects are evidenced beyond 170 msec post-stimulus.

DISCUSSION

There is convergence of results to suggest that neural processes of the centromedian region contribute to the sensory responses recorded from the postcruciate cortex. Both the unit data and evoked potentials recorded simultaneously from the same micro-electrode show modified responses during cooling of the CM region. The magnitude of the changes caused by thalamic cooling was substantial. For example, the conservative measure of the area under the rectified AEP showed an average 30% decrement during bilateral cooling for ipsilateral paw stimulation. Significant changes resulting from cooling CM region were also found for responses evoked by light or contralateral hindpaw stimulation, and for the unit data.

The cooling effect cannot be attributed to blockade of the specific somatic pathway. A recording was made from nucleus ventralis posterior lateralis, and no significant impairment was evidenced anterior to the cooling blockade. A specific pathway interpretation would not be an appropriate explanation for the effect of cooling on light elicited responses. Furthermore, the response interval analysis for somatic stimulation (Figure 15) indicates that there is an absence of cooling influence on the short latency primary response. The histogram of Figure 7 depicts the relative stability of the primary response through all cooling conditions, whereas a longer latency component, approximately 50 through 100 msec, is virtually abolished.

It is most likely that the neural processes of the centra median region contributing to sensory responses of the postcruciate cortex are synaptic processes rather than fibers of passage. According to

Benita and Conde (6), it is possible to differentiate fiber blockade from synaptic blockade according to the temperature of cooling. At 5° C it is most likely that the functional blockade was restricted to synaptic processes and large fibers immediately adjacent to the probe tip. Parametric data from the literature indicate that blockade of conduction along small fibers would be unlikely (6, 15, 24). Given a 5° C tip temperature and a 6° C/mm temperature gradient (20), it is reasonable to assume a volumetric blockade of synaptic activity extending about 2.5 mm from the probe tip. These dimensions are based upon a 20° C upper limit for synaptic blockade (6). Consequently, bilateral cooling to 5° C would block synaptic activity throughout nucleus centromedian and would extend well into nucleus parafascicularis according to standard probe placement.

Since functional blockade includes the entire CM region, one would expect the complete abolition of sensory input contributed through this area. In some cases this situation is evident in the unit post-stimulus histogram. The effect of bilateral cooling virtually abolishes the unit response, as might be expected if the predominant sensory input for the neuron is contributed from CM region. An example of such a histogram may be seen in Figure 5. This result is consistent with the findings of Blum et al. (8). They found neurons of the postcruciate cortex which would invariably respond to CM stimulation, which were unaffected by VL stimulation. However, more typically, bilateral cooling, rather than abolishing the unit response, caused a partial decrement of the unit response. Such cells would appear to be characterized by additional sensory input pathways. Substantiating evidence comes from the finding

that CM stimulation often evoked unit activity in the postcruciate cortex that could also be evoked by stimulation of either of the ventrolateral nucleus of the thalamus or the primary sensory receiving area (8).

Although the average decrease in unit response firing rate was about 50%, the individual cells ranged from nearly 100% response abolition to those only marginally altered by bilateral cooling. Possible functional pathways would include conduction through the dorsal leaf of the nonspecific thalamic bifurcation with small fibers extending anteriorly well beyond CM. Such small fiber conduction would be more resistant to the cooling blockade than synaptic processes, and if terminating sufficiently anterior to CM these small fibers could maintain an undisrupted sensory input. Experimentally a comparison of the effects on unit responses of a cryoprobe blockade adjacent to the inferior thalamic peduncle (ITP) would allow an evaluation of the dorsal leaf contribution by-passing the CM blockade. For example, Skinner found that ITP blockade consistently enhanced the short latency visual evoked potential (45). In contrast, CM blockade resulted in enhancement of about 25% of the visual evoked potentials, and the magnitude of effect was not as great as that reported for ITP blockade.

The functional pathway through the ventral leaf would remain intact during CM cooling, the bifurcation being posterior to the cooling blockade. The manner in which ascending projections of the ventral route might reach the postcruciate cortex have not been clarified, but fibers from the ventral route do reach the dorsomedial nucleus via the hypothalamus (36). The observed desynchronization of the cortical EEG suggests that the ventral route has been unimpaired during thalamic cooling (39).

Considering the existence of various afferent pathways to the sensorimotor cortex, it is possible that the magnitude of unit response decrement resulting from cooling reflects the balance between sensory input coursing through the CM region with that of alternate pathways.

The data consistently showed the most pronounced cooling effects to result from bilateral cooling rather than unilateral cooling. The greater effectiveness of bilateral cooling was evident in all cases, for all three stimuli and for the unit data as well as the evoked potential data. The greater superiority of bilateral cooling when compared with unilateral cooling is clearest for somatic stimuli. For somatic stimuli, the bilateral cool condition is significantly more effective in reducing the excitatory unit response data and in decreasing the AEP area than the unilateral cooling condition. For the AEP area data, the difference between unilateral cooling and bilateral cooling is significant at the .005 level. For example, the least significant difference was between the bilateral cool condition and contra cool condition for the contralateral hindpaw group, and even this difference was highly significant statistically (paired t-value of 3.49, 26 df, $p < .005$).

For some of the somatic data it appears as if the average effect of bilateral cooling is the additive sum of ipsilateral cooling plus contralateral cooling. For example, the excitatory unit responses elicited by ipsilateral paw stimulation reflects the summation phenomenon. Ipsilateral cooling decreases the spike rate an average of 4 spikes/sec, contralateral cooling decreases the rate by 4 spikes/sec, and bilateral cooling decreases the spike rate 8 spikes/sec.

The ipsilateral paw AEPs show the same additive effect for the area analysis. Ipsilateral cool decreases the area 15%, contralateral cool decreases the area 18%, and bilateral cooling decreases the area 30%. Thus, in the cat stimulation of the ipsilateral hindpaw results in bilateral elicited activity at the level of the thalamic area of centromedian. Since blocking activity of either hemisphere decreases the sensory evoked responses in the postcruciate cortex, a pathway must exist in which information from the contralateral centromedian nucleus reaches the postcruciate cortex. The findings of Albe-Fessard and Rougeul suggest that the route from the contralateral CM to the cortex is not transcallosal. (2)

The contralateral paw data, both for the excitatory unit response and the AEP area analysis, show that the effect of bilateral cooling approximates the simple sum of ipsilateral and contralateral cooling conditions. Ipsilateral cooling decreases the excitatory unit response by an average of 5 spikes/sec, contralateral cooling decreases the rate by 4 spikes/sec, and bilateral cooling decreases the rate by 8.5 spikes/sec. A similar pattern exists for the contralateral paw AEP area data.

Thus, on the basis of physiological evidence, it appears as if the influence from either the ipsilateral or contralateral CM to the postcruciate cortex is approximately equal. This findings contrasts with that of Skinner and Lindsley who suggested a predominant ipsilateral relationship between the inferior thalamic peduncle and the orbitofrontal cortex (43).

In distinction, the bilateral cool effect does not approximate the sum of both unilateral cool conditions for the light stimulus data, whether AEP or unit recordings. Similarly, bilateral cooling is not simply additive for the somatic inhibitory unit data and AEP peak-to-peak analysis.

Peak-to-peak and area analysis

It is perhaps worthwhile to consider the differences between the area analysis and peak-to-peak measure for the somatic stimuli. The area analysis is a conservative measure of the cooling effect. There is no interval selection, and no possibility of experimenter bias. The measure extends for 0.5 sec post-stimulus, and exhibits almost total recovery.

In contrast, the peak-to-peak analysis measures a restricted portion of the evoked potential, perhaps 20 msec. The peak-to-peak amplitude measure considers the positive and negative components of the evoked potential, unlike the area analysis which has been rectified to yield the absolute value.

The peak-to-peak measure of the amplitude of AEP components reflects both the synchronized discharge of the neural processes which give rise to the evoked potential and, the number or quantity of discharging elements. Similarly the area analysis would represent the number of discharging bioelectric elements yielding the evoked potential, however, this measure would be less critically dependent upon the synchrony of discharge. As evidenced from the somatic stimulation data, it is apparent that the greatest magnitude of cooling effect is upon

the peak-to-peak measure rather than the area measure. Since the magnitude of the peak-to-peak measure, which is dependent on the close temporal coincidence of neural processes which lead to the AEP, is predominantly affected, it is suggestive to characterize the cooling impairment to be predominantly a deficit in the synchrony of neural processes. However, the effect of bilateral cooling of the CM region is not confined to a synchrony deficit. If only the synchrony of discharge were influenced by cooling with the same number of neural elements discharging over a longer span of time, then a decrease in the peak-to-peak amplitude would be expected, with no change in the area circumscribed by the waveform. In distinction, this situation does not describe the results of bilateral thalamic cooling. Consequently, the cooling results seem to suggest that both the quantity and synchrony of the neural processes giving rise to the AEP are influenced by bilateral cooling of CM region. According to the greater magnitude of effect, the predominant impairment resides within the synchronization of activity.

The consideration of the peak-to-peak measure and the area measure as indexing two different phenomena is most intriguing when contrasting the effects of unilateral cooling. As has been discussed previously, the unilateral cooling effect using the area AEP analysis for somatic stimuli can best be described as being simply additive in achieving the effect during bilateral cooling. It appears as if the unilateral cooling effect is approximately 50% of the bilateral cool condition, and that the sum of the ipsilateral cooling effect plus the contralateral cooling effect yields the bilateral cooling effect. Although this describes the cooling effects for the area analysis for somatic stimuli, this is not

true for the peak-to-peak analysis. Unlike the area measure, the peak-to-peak measure shows a substantially greater effect from ipsilateral cooling than contralateral cooling. This applies for both the contralateral hindpaw stimulation and ipsilateral hindpaw stimulation data. In the latter case, the ipsilateral cooling effect is significantly greater than the contralateral cooling effect, the chance probability level being less than .01, and ipsilateral cooling accounts for almost the entire effect of bilateral cooling.

It is interesting to consider the possibility that the contrast in results caused by unilateral cooling reflects the different processes measured by the two methods of AEP analysis, the area measure and the peak-to-peak measure. In viewing the peak-to-peak amplitude measure as an index of synchrony, one might postulate that the neural circuitry subserving the synchronizing process is related ipsilaterally between the non-specific thalamus and postcruciate cortex. This would account for the great deficit in peak-to-peak amplitude achieved by ipsilateral cooling.

It is possible that the area analysis of the AEP reflects primarily the quantity or volume of neural elements yielding the evoked potential, thus the area measure might index post-synaptic potential power, both excitatory and inhibitory post-synaptic potentials. There appears to be an almost equal contribution from either side of the nonspecific thalamus to the area of the AEP recorded in the postcruciate cortex. This might be interpreted as resulting from the functional blockade of a finite amount of neural activity which would ordinarily contribute to the cortical evoked potential. Consequently bilateral cooling, which

would cause the functional blockade of twice the neural volume, results in a decrease in post-synaptic potential power which is the additive sum of ipsilateral and contralateral cooling.

Unit somatic response data

Single units recorded from postcruciate cortex showed response decrements during reversible cooling of the CM region. It appears as if the influence of cooling is most clearly tied to modifying the post-stimulus rate. In contrast, the pre-stimulus rate, or background level of spontaneous unit activity, is little affected by the cooling conditions. The negative finding with respect to the influence of cooling on the pre-stimulus rate is illustrated in Figure 4. Although a slight change in the pre-stimulus rate is evidenced, the magnitude of change is not statistically significant. Consequently the unit results have been described as a difference score, the post-stimulus mean rate minus the pre-stimulus mean rate, which would obviate any fluctuations in the background rate, while accurately describing the elicited response.

It was found that cooling of the CM region affected both the excitatory and inhibitory components of the elicited response. This was true for both the somatic and visual stimuli. However, some differences are evident in the empirical results contrasting the excitatory and inhibitory response components.

The pattern of cooling effects for the excitatory unit responses to somatic stimuli appears analogous to the AEP area analysis. The results of either ipsilateral or contralateral cooling are virtually identical in magnitude. Similarly the sum of the unilateral cooling effects closely approximates the bilateral cooling effect. This

clearly suggests a bilateral convergence of sensory input from the non-specific thalamus to the postcruciate cortex. Since a dominance of laterality was not exhibited for the unilateral cooling effects which was comparable to the AEP analysis, it is reasonable to invoke a similar explanation. The unit response decrement might reflect the volumetric blockade of CM synaptic activity and the ensuing decrease of cortical post-synaptic potentials which would ordinarily contribute to the unit response. The larger the blockade, as in bilateral cooling, the larger the decrement in post-synaptic potentials.

Light elicited responses

The effect of thalamic cooling upon sensory responses recorded in the postcruciate cortex differs for light elicited responses from somatic responses. The light elicited unit response is quite weak in contrast with the somatic data. It is interesting that any cooling, whether unilateral of bilateral, is sufficient to severely reduce the responses elicited by light. In contrast with the somatic data, bilateral cooling is not significantly more effective in reducing the unit response than ipsilateral cooling. It appears as if both the excitatory and inhibitory unit responses elicited by light are easily disrupted and subject to virtual abolition by any thalamic cooling.

The effect of thalamic cooling upon the averaged evoked potentials elicited by the light flash differed from those elicited by paw stimulation. Unlike the latter, the light stimulus AEPs fall into two categories, those enhanced in amplitude and area and those decreased. For example, the recorded AEPs associated with a single unit often showed enhancement during thalamic cooling for light stimuli, but a

reduction for somatic stimuli. Over 40% of the light AEPs showed enhancement in area during cooling. In attempting to account for the direction of the change in response, the variables of cryoprobe location, recording electrode depth, and the particular cats were examined. No correlation was found between these variables and the occurrence of response increases or decreases.

The somatic AEP data show partial effects with unilateral cooling. The light AEP data show comparable effects of any type of cooling, whether ipsilateral, contralateral, or bilateral; this is most evident from the area analysis. As was the case for the light elicited unit responses, the light AEP is much smaller in amplitude than the somatic response. Assuming that bilateral cooling abolishes the sensory response coursing through the CM region, it appears as if the magnitude of the contribution through CM region is perhaps one-fifth of the post-synaptic potential power that yields the area under the recitified light AEP.

Although we are dealing with the non-specific sensory system in the CM region, it is evident that the effect of this functional blockade on light responses differs from that for somatic responses and is not truly non-specific. Perhaps the clearest distinction is evidenced from the characterization of the portion of the response most affected by cooling, accomplished through the interval analysis.

Interval analysis

It has been reported that the short latency components of the AEP are primarily attributed to the specific sensory pathways while the longer latency intervals, beyond 80 msec, are contributed by the reticular formation and collaterals extending from the reticular

formation (22, 23, 48). Accordingly, the somatic stimuli and light stimuli have been compared as to the portion of the response most affected by blockade of the CM region. Through the interval analysis it was apparent that the longer latency portions of the response are most often influenced during cooling. The histograms for both ipsilateral paw stimulation and contralateral paw stimulation showed the predominant effect within about 100 through 200 msec post-stimulus. However, the light stimulus histogram differs from that for the somatic stimuli. When cooling yielded a decrement in the light stimulus AEP area, the portion of the response most influenced was diffuse rather than well confined. The portion influenced was somewhat centered toward the longer latency part of the response, about 200 msec post-stimulus, although affected intervals extended to almost 500 msec post-stimulus. In contrast with the somatic data, a sub-group was distinguished which showed enhancement of AEP area during cooling. Further credence for distinguishing these groups, is apparent from the corresponding interval analysis. The enhancement effect was found to be well centered at about 50 msec, and was significantly different from those light responses which decreased. These distinct interval histograms suggest two distinct phenomena resulting from bilateral thalamic cooling.

One phenomenon, reflecting the early latency enhancement, suggests an interaction between the specific sensory pathway and the non-specific system. For the visual system such an interaction might occur at the level of the lateral geniculate, receiving fibers from the non-specific thalamic nuclei via nucleus reticularis (37). The non-specific system

might act with a tonic inhibitory input to the specific pathway. A functional blockade of the non-specific thalamic nuclei, in suspending the tonic inhibition, could yield an enhancement of the early portion of the AEP. This early latency enhancement of the visual AEP is consistent with the finding of Skinner and Lindsley, who found consistent enhancement of the visual evoked potential during blockade of the inferior thalamic peduncle (45).

The second phenomenon resulting from bilateral thalamic cooling affects the longer latency components. Skinner and Lindsley did not report on these affects of thalamic cooling. Beyond 80 msec post-stimulus, there is a decrement of the non-specific sensory response recorded in the cortical AEP. The pathway, projecting from the non-specific thalamic nuclei to the cortex, reflects the decreased post-synaptic potential power resulting from the functional blockade. It appears as if a longer latency phasic input to the postcruciate cortex has been interrupted. It is interesting to compare the portion of the response most affected by bilateral cooling with the recruiting response data and the time course of inhibitory post-synaptic potentials recorded from the non-specific thalamus.

The results of numerous studies confirm a critical rate of repetitive stimulation at 5-12/sec for eliciting recruiting responses (18, 24, 47). This repetitive rate and the recruiting response seem related to the role of the non-specific thalamus acting to synchronize neural activity. The synchronizing function of the non-specific thalamus is evidenced both by the enhancement of the large amplitude cortical waves during repetitive stimulation of the midline thalamus, and from

spontaneous sleep spindles appearing in a variety of comatose p[illegible]-ations (14, 47).

It is noteworthy that the cooling effects are predominantly effective in reducing the peak-to-peak amplitude of the cortical AEP, a measure that reflects synchronous activity. It is interesting to consider that recruiting demands a repetitive rate corresponding to an 80 through 200 msec interstimulus interval. This, in fact, closely describes that portion of the response most affected by bilateral cooling.

Purpura recorded the time course of inhibitory post-synaptic potentials from the midline thalamus (33, 34). It is interesting that the latency of the IPSPs is quite comparable with that of the portion of the response blocked by bilateral cooling. It is suggestive to consider the non-specific thalamus as performing a frequency gating role. The frequency is established by the IPSP phasing at approximately 100 msec. A single somatic stimulus yields a primary response, unimpaired by thalamic cooling, at a latency shorter than 50 msec. This single stimulus is sufficient to create IPSP phasing by the arrival of neural activity through the reticular formation through to the non-specific thalamic nuclei. The functional blockade of the CM region consequently shows its predominant effect through the loss of the IPSP phasing; the somatic response interval most affected is from 100 to 200 msec post-stimulus.

The importance of the non-specific thalamic nuclei in cortical synchrony is evident from EEG studies (12). Skinner has shown the abolition of spontaneous sleep spindles during blockade of the non-specific thalamus (41, 43). To evaluate this possibility a cortical

screw was lowered to the dura above the suprasylvian gyrus. The polygraph record showed a prevalence of desynchronized low voltage fast EEG activity which was present before, during, and after cooling. Only occasionally were sleep spindles present, and it was not possible to determine whether the cooling of CM region blocked the spindles.

SUMMARY AND CONCLUSIONS

This study endeavored to examine sensory evoked responses contributed through the non-specific thalamus to the postcruciate cortex. To achieve this purpose, single units and focal evoked potentials were recorded from the postcruciate cortex of acutely prepared cats. Neural activity of the caudal non-specific thalamus (centromedian-parafascicular complex) was blocked by a reversible cryogenic lesion. The placement of the cryoprobes was verified histologically. The stimuli examined were subcutaneous shock to the ipsilateral and contralateral hindlimb and light flash.

Evaluation of the cooling effect was based on post-stimulus histograms and averaged evoked potentials summed from 100 stimulus presentations. Using an electrode positioned in nucleus ventralis posterior lateralis (VPL), it was shown that the cryogenic lesion did not extend into the somatic primary afferent system since the short latency response recorded from VPL was unaffected.

Thalamic cooling had relatively little influence on the pre-stimulus spike frequency of postcruciate units. In contrast, the responses elicited by the light stimulus or somatic stimuli were substantially reduced during thalamic cooling. The greatest changes were evident during bilateral thalamic cooling. Partial decreases in the elicited unit response resulted from either ipsilateral or contralateral cooling. The extent of change in spike frequency found during thalamic cooling ranged widely across cells. The extremes ranged from the almost total abolition of the elicited response to almost no change from the pre-cool control response. Frequently, the spike frequency changed from the pre-cool control by about 50% during bilateral thalamic cooling.

The decrease in sensory responses applied to both excitatory responses, those above the background level, and inhibitory responses, those below the background level. In the former, thalamic cooling decreased the mean spike rate, while in the latter, thalamic cooling increased the mean spike rate toward the background rate. The influence of thalamic cooling was to decrease the magnitude of the elicited response, whether excitatory or inhibitory, and was shown for all stimuli tested.

The analysis of the focal evoked potentials recorded in the postcruciate cortex showed decreases in the peak-to-peak amplitude and area under the averaged evoked potential for somatic stimuli during thalamic cooling. The magnitude of change was greatest for the peak-to-peak measure.

Unlike the somatic stimuli, the light evoked potentials sometimes showed enhancement during thalamic cooling. An interval analysis examined the portion of the response influenced by thalamic cooling. It was shown that the light evoked potentials were enhanced during the earlier latencies, and were diminished during the longer latencies. A descriptive histogram was formed of the response intervals affected by thalamic cooling. The interval histograms for ipsilateral and contralateral hindpaw stimulation were similar, while the light stimulus histograms differed.

It was concluded that the centromedian thalamic area contributes importantly to sensory responses in the postcruciate cortex. Following electrical stimulation of the hindpaw, neurons in the postcruciate cortex initially receive neural input ascending via the medial lemniscus

and VPL. This results in the first wave of activity, shorter than 30 msec in latency. The peripheral stimulus also elicits neuronal activity in the CM area of the non-specific thalamus via multineuronal pathways. Impulses arriving in CM elicit long lasting inhibitory post-synaptic potentials, which act to synchronize impulses ascending from CM to the cortex. The particular synchronization of neural activity is based upon the duration of the IPSPs and is approximately 100 msec. At about 100 msec post-stimulus, a wave of impulses reach the post-cruciate cortex from CM. Blocking neural activity in the CM area particularly impairs this longer latency neural activity from effectively contributing to the sensory response in the postcruciate cortex. In this manner, the centromedian thalamic area influences both excitatory and inhibitory cortical sensory responses. An alternative conception is that CM would act to provide a relatively stable input to cortical neurons, an input necessary for the complete development of the response. However, the slight effect of CM blockade upon the pre-stimulus mean rate makes this interpretation unlikely.

REFERENCES

1. Albe-Fessard, D., and Fessard, A. Thalamic integrations and their consequences at the telencephalic level. Progr. Brain Res., 1963, 1, 115-148.

2. Albe-Fessard, D., and Rougeul, A. Activites d'origine somesthesique evoquees sur le cortex nonspecifique du chat anesthesie au chloralose: role du centre median du thalamus. Electroenceph. clin. Neurophysiol., 1958, 10, 131-152.

3. Andersen, P., Andersson, S. A., and Lomo, T. Some factors involved in the thalamic control of spontaneous barbiturate spindles. J. Physiol., 1967, 192, 257-281.

4. Ballantine, H. T., Bell, E., Manlapaz, J. Progress and problems in the neurological applications of focused ultrasound. J. Neurosurg., 1960, 17, 858-863.

5. Benita, M., and Conde, H. Etude des efferences du noyau centre median du thalamus du chat vers le cortex et les structures striopallidales. Exp. Brain Res., 1971, 12, 204-222.

6. Benita, M., and Conde, H. Effects of local cooling upon conduction and synaptic transmission. Brain Res., 1972, 36, 133-151.

7. Benita M., and Conde, H. Reversible blockage of specific synaptic transmission by localized and moderate cooling with a vacuum insulated probe connected to a closed circuit apparatus. Confin. neurol., 1972, 34, 218-223.

8. Blum, B., Halperin, L. M., and Ward, A. A. Microelectrode studies of the afferent connections and efferent projections of neurons in the sensorimotor cortex of the cat. Exptl. Neurol., 1968, 20, 156-173.

9. Bowsher, D. Some afferent and efferent connections of the para-fascicular-center median complex. In D. P. Purpura and M. D. Yahr (Eds.), The thalamus. New York: Columbia Univ. Press, 1966, pp. 99-108.

10. Bowsher, D., Mallart, A., Petit, D., and Albe-Fessard, D. A bulbar relay to the centre median. J. Neurophysiol., 1968, 31, 288-300.

11. Brodal, A. Neurological anatomy (2nd ed.). New York: Oxford Univ. Press, 1969 (pp. 326-335).

12. Buser, P., and Horvath, F. E. Thalamocaudate-cortical relationships in synchronized activity. II. Further differentiation between spindle systems by cooling and lesions in the mesencephalon. Brain Res., 1972, 39, 43-60.

13. Buser, P., and Imbert, M. Sensory projections to the motor cortex in cats. In Rosenblith, W. A. (Ed.), Sensory communication. Cambridge: M.I.T. Press, 1961 (pp. 607-626).

14. Dahl, E., Gjerstad, L. I., and Skrede, K. K. Persistent thalamic and cortical barbituate spindle activity after ablation of the orbital cortex in cats. Electroenceph. clin. Neurophysiol., 1972, 33, 485-496.

15. Denny-Brown, D., Adams, R. D., Bremer, C., and Doherty, M. M. The pathology of injury to nerve induced by cold. J. Neuropath. Exp. Neurol., 1945, 4, 305-323.

16. Dondey, M., Albe-Fessard, D., and Le Beau, J. Premieres applications neurophysiologiques d'une methode permettant le blocage electif et reversible de structures centrales par refrigeration localisee. Electroenceph. clin. Neurophysiol., 1962, 14, 758-763.

17. Horvath, F. E., and Buser, P. Thalamo-caudate-cortical relationships in synchronized activity. I. Differentiation between ventral and dorsal spindle systems. Brain Res., 1972, 39, 21-41.

18. Jasper, H. H. Unspecific thalamocortical relations. In J. Field (Ed.), Handbook of Physiology. Vol. II Neurophysiology. Baltimore: Waverly Press, 1960 (1307-1322).

19. Jasper, H. H., and Ajmone-Marsan, C. A stereotaxic atlas of the diencephalon of the cat. Ottawa: National Research Council of Canada, 1954.

20. Jasper, H. H., Shacter, D. G., and Montplaisir, J. The effect of local cooling upon spontaneous and evoked electrical activity of the cerebral cortex. Can. J. Physiol. Pharmacol., 1970, 48, 640-652.

21. Krupp, P., and Monnier, M. The unspecific intralaminary modulating system of the thalamus. Int. Rev. Neurobiol., 1966. 9, 45-94.

22. Lewis, E. G., Dustman, R. E., and Beck, E. C. The effects of alcohol on visual and somato-sensory evoked responses. Electroenceph. clin. Neurophysiol., 1970, 28, 202-205.

23. Lindsley, D. B. Electrophysiology of the visual system and its relation to perceptual phenomena. In M. A. Brazier (Ed.), Brain and behavior. Washington: Amer. Inst. Biol. Sci., 1961, (pp. 359-392).

24. Lundberg, A. Potassium and the differential thermosensitivity of membrane potential, spike and negative afterpotential in mammalian A and C fibres. Acta. Physiol. Scand., 1948, 15, Suppl. 50.

25. Mark, V. H., Chato, J. C., Forest, G. E., and Aronow, S. Localized cooling in the brain. Science, 1961, 134, 1520-1521.

26. Mehler, R. Further notes on the center median nucleus of Luys. In D. P. Purpura and M. D. Yahr (Eds.), The thalamus. New York: Columbia Univ. Press, 1966 (pp. 109-128).

27. Morison, R. S., and Dempsey, E. W. A study of thalamo-cortical relations. Amer. J. Physiol., 1942, 135, 281-292.

28. Moseley, J. I., Ojemann, G. A., and Ward, A. A. Unit activity during focal cortical hypothermia in the normal cortex. Exptl. Neurol., 1972, 37, 152-163.

29. Mountcastle, V. B. Structural organization and general physiology of thalamotelencephalic systems. In V. B. Mountcastle (Ed.), Medical Physiology (12th Ed.). St. Louis: C. V. Mosby, 1968, (vol. 2, pages 1277-1314).

30. Nauta, W. J. H., and Whitlock, D. G. An anatomical analysis of the non-specific thalamic projection system. In J. F. Delafresnaye (Ed.), Brain mechanisms and consciousness. Springfield: Charles C. Thomas, 1954 (pp. 81-116).

31. O'Brien, J. H., and Fox, S. S. Single cell activity in cat motor cortex. I. Modifications during classical conditioning procedures. J. Neurophysiol., 1969, 32, 267-284.

32. O'Brien, J. H., and Fox, S. S. Single cell activity in cat motor cortex. II. Functional characteristics of the cell related to conditioning changes. J. Neurophysiol., 1969, 32, 285-296.

33. Purpura, D. P. Operations and processes in thalamic and synaptically related neural subsystems. In F. O. Schmitt (Ed.), The neurosciences, 2nd study program. New York: Rockefeller Univ. Press, 1970 (pp. 458-470).

34. Purpura, D. P., and Shofer, R. J. Intracellular recording from thalamic neurons during reticulocortical activation. J. Neurophysiol., 1963, 26, 494-505.

35. Scheibel, M. E., and Scheibel, A. B. Patterns of organization in specific and nonspecific thalamic fields. In D. P. Purpura and M. D. Yahr (Eds.), The thalamus. New York: Columbia Univ. Press, 1966 (pp. 13-46).

36. Scheibel, M. E., and Scheibel, A. B. Structural organization of nonspecific thalamic nuclei and their projection toward cortex. Brain Res., 1967, 6, 60-94.

37. Scheibel, M. E., and Scheibel, A. B. Elementary processes in selected thalamic and cortical sybsystems - the structural substrates. In F. O. Schmitt (Ed.), The neurosciences, 2nd study program. New York: Rockefeller Univ. Press, 1970 (pp. 443-457).

38. Skinner, J. E. A cryoprobe and cryoplate for reversible functional blockade in the brains of chronic animal preparations. Electroenceph. clin. Neurophysiol., 1970, 29, 204-205.

39. Skinner, J. E. Electrocortical desynchronization during functional blockade of mesencephalic reticular formation. Brain Res., 1970, 22, 254-258.

40. Skinner, J. E. Abolition of a conditioned, surface negative, cortical potential during cryogenic blockade of the nonspecific thalamo-cortical system. Electroenceph. clin. Neurophysiol., 1971, 31, 197-209.

41. Skinner, J. E. Abolition of several forms of cortical synchronization during a blockade in the inferior thalamic peduncle. Electroenceph. clin. Neurophysiol., 1971, 31, 211-221.

42. Skinner, J. E. Neuroscience: A laboratory manual. Philadelphia: W. B. Saunders, 1971 (pp. 163-193).

43. Skinner, J. E., and Lindsley, D. B. Electrophysiological and behavioral effects of blockade of the nonspecific thalamo-cortical system. Brain Res., 1967, 6, 95-118.

44. Skinner, J. E., and Lindsley, D. B. Reversible cryogenic blockade of neural function in the brain of unrestrained animals. Science, 1968, 161, 595-597.

45. Skinner, J. E., and Lindsley, D. B. Enhancement of visual and auditory evoked potentials during blockade of the non-specific thalamo-cortical system. Electroenceph. clin. Neurophysiol., 1971, 31, 1-6.

46. Snider, R. S., and Niemer, W. T. A stereotaxic atlas of the cat brain. Chicago: Univ. of Chicago Press, 1961.

47. Spencer, W. A., and Brookhart, J. M. Electrical patterns of augmenting and recruiting waves in depths of sensorimotor cortex of cat. J. Neurophysiol., 1961, 24, 26-49.

48. Towe, A. L. Electrophysiology of the cerebral cortex: consciousness. In T. C. Ruch and H. D. Patton (Eds.), Physiology and biophysics. Philadelphia: Saunders, 1965 (pp. 458-462).

49. Tyner, C. F., and Towe, A. L. Interhemispheric influences on sensorimotor neurons. Exptl. Neurol., 1970, 28, 88-105.

50. Walker, A. E. Internal structure and afferent-efferent relations of the thalamus. In D. P. Purpura and M. D. Yahr (Eds.), The thalamus. New York: Columbia Univ. Press, 1966 (pp. 1-12).